Crustal structure beneath the Trøndelag Platform and adjacent areas, mid-Norwegian margin, derived from wide-angle seismic and potential field data – Supplementary material

Asbjørn Johan Breivik [a,*] Rolf Mjelde [b] Thomas Raum [b]
Jan Inge Faleide [a] Yoshio Murai [c] Ernst R. Flueh [d]

[a]*Department of Geosciences, University of Oslo, PO Box 1047, Blindern, 0316 Oslo, Norway*

[b]*Department of Earth Science, University of Bergen, Allegt. 41, 5007 Bergen, Norway*

[c]*Institute of Seismology and Volcanology, Hokkaido University, Sapporo 060, Japan*

[d]*IFM-Geomar, Leibniz-Institute for Marine Sciences, Wischhofstr. 1-3, 24148 Kiel, Germany*

Introduction

This document contains supplementary material to the main article, documenting the complete wide-angle seismic data set, interpretation, ray tracing models, and travel-time fit. For completeness and context, some figures from the main paper are repeated here. The data is presented in the same sequence as it is discussed in the paper. Profile location is shown in Fig. 1, instrument locations in Fig. 2. Seismic phases constraining the crystalline crust are indicated for each data set (P_{g1}: upper basement refractions, P_{g2} and P_{g3}: middle crustal refractions, P_{g4}: lower crustal refractions, $P_M P$: reflections off the Moho).

The processing of the data consists of de-biasing, band-pass filtering (6 to 12 Hz), spiking predictive deconvolution, and amplitude gain scaling (AGC). The P-wave data is velocity reduced by 8.0 km s^{-1}. The first shots were not recorded by the land stations because they were not in place before after the shooting commenced. Most land stations can record offsets up to 150-200 km, which appears adequate compared to the OBS/H station coverage.

* Corresponding address: Department of Geosciences, University of Oslo, PO Box 1047, N-0316 Oslo, Norway

Email address: a.j.Breivik@geo.uio.no (Asbjørn Johan Breivik).
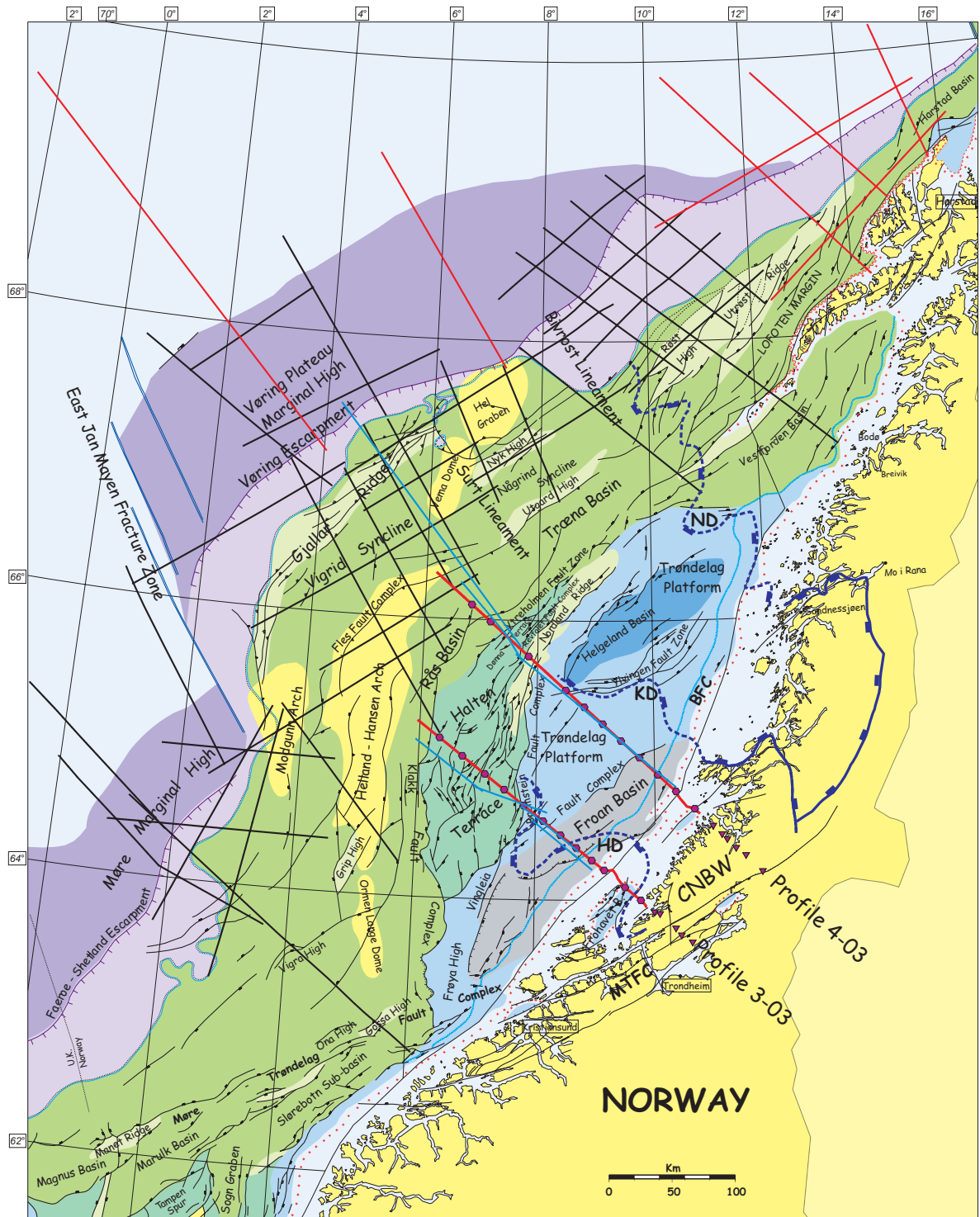
Fig. 1. The study area across the Trøndelag Platform, off mid-Norway. The shot lines of Profile 3-03 and 4-03 discussed in the paper are shown as bold red lines with purple hexagons marking OBS/OBH receiver positions, inverted triangles marks the land stations. Other OBS/H profiles from the Euromargins 2003 survey are shown by red lines, older surveys by black lines. The geological base map is from Blystad et al. (1995), while the proposed offshore continuations of the Kollstraumen and Nesna Detachments are from Olesen et al. (2002), and the Høybakken Detachment from Skilbrei et al. (2002). CNBW: Central Norway Basement Window, HD: Høybakken Detachment, KD: Kollstraumen Detachment, ND: Nesna Detachment.

2
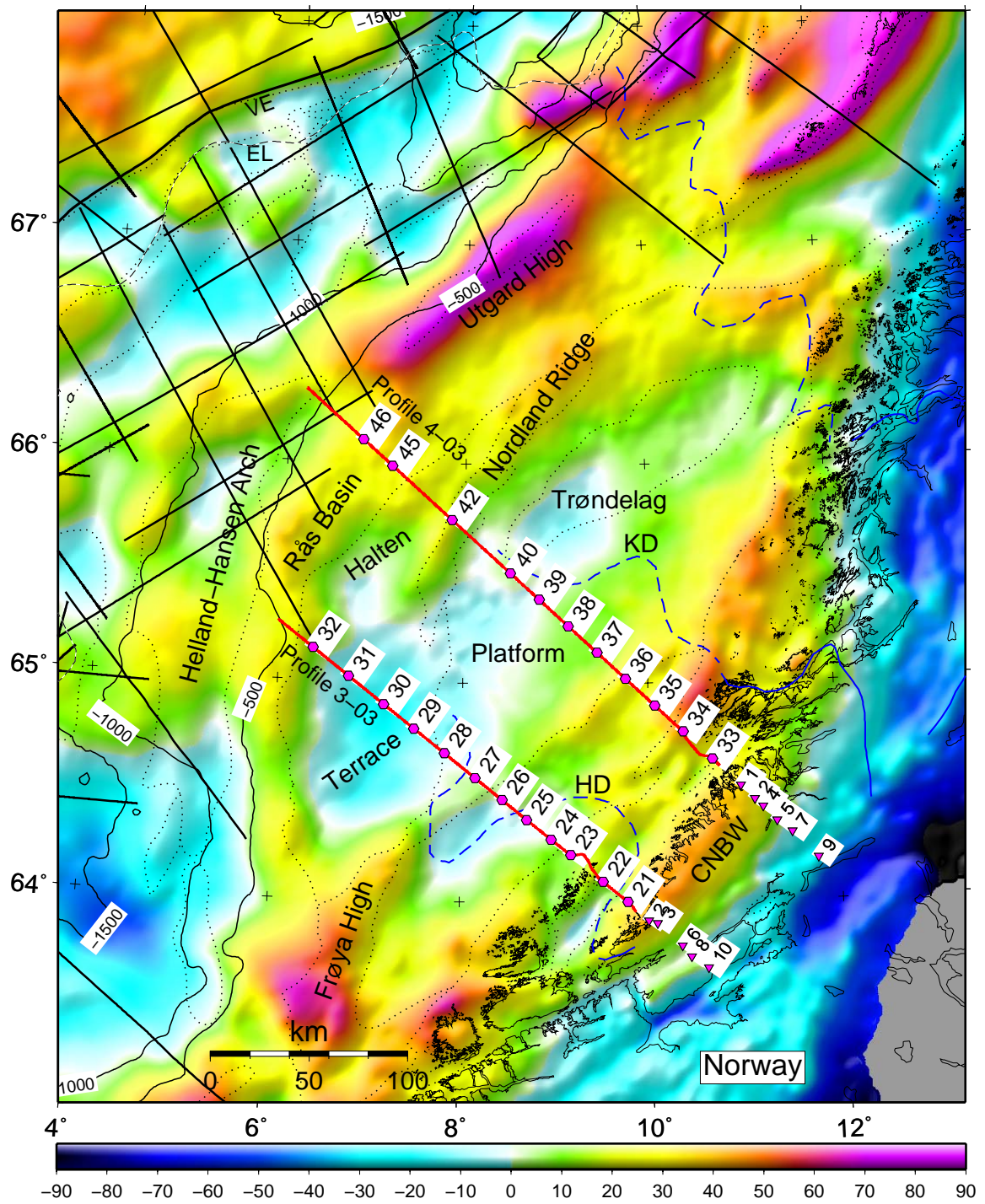
Fig. 2. Gravity map based on ERS-1 and Geosat satellite data, ship track data, and land measurements (Skilbrei et al., 2000). Offshore gravity is Free-Air, onshore data is Bouguer corrected (density 2670 kg m^{-3}). Survey navigation with instrument positions are shown in red, other OBS survey navigation in black. The 500, 1000, and 1500 m bathymetry contours are also shown together with proposed offshore extensions of detachments (Skilbrei et al., 2002; Olesen et al., 2002). Shaded relief is illuminated from the NW. CNBW: Central Norway Basement Window, EL: Eastern limit lava flows, VE: Vøring Escarpment. Outlines of structural elements (dotted) are from Blystad et al. (1995) (Fig. 1).

Profile 4-03

The profile has data from 11 OBS/Hs and 6 land seismometers (Figs. 3–19). These are OBS/Hs 33-40, 42, 45, 46, and land stations 1, 2, 4, 5, 7, 9. Data and models are presented from NW to SE, starting with OBS 46. The velocity model used for the ray tracing is shown in Fig. 20.
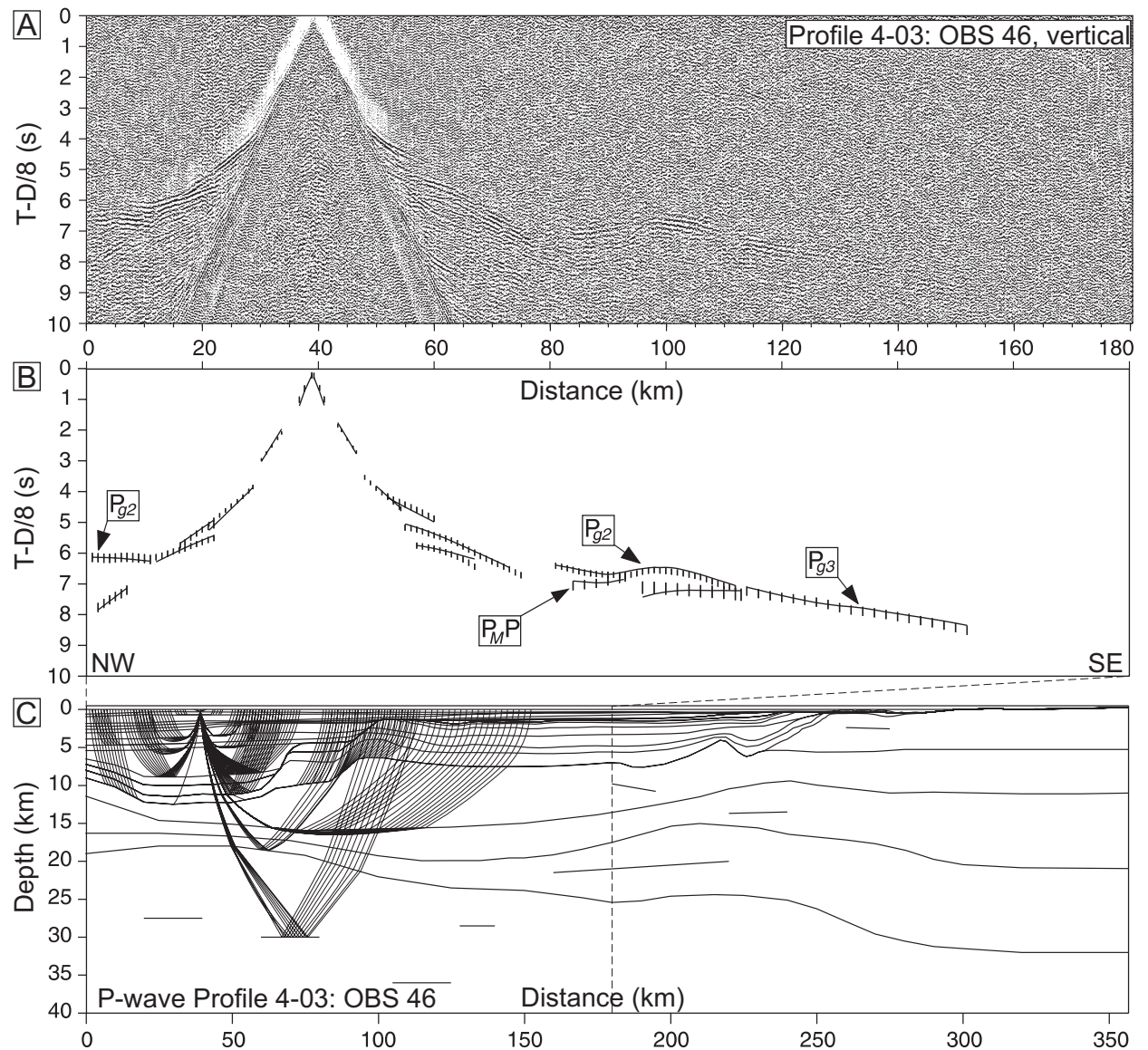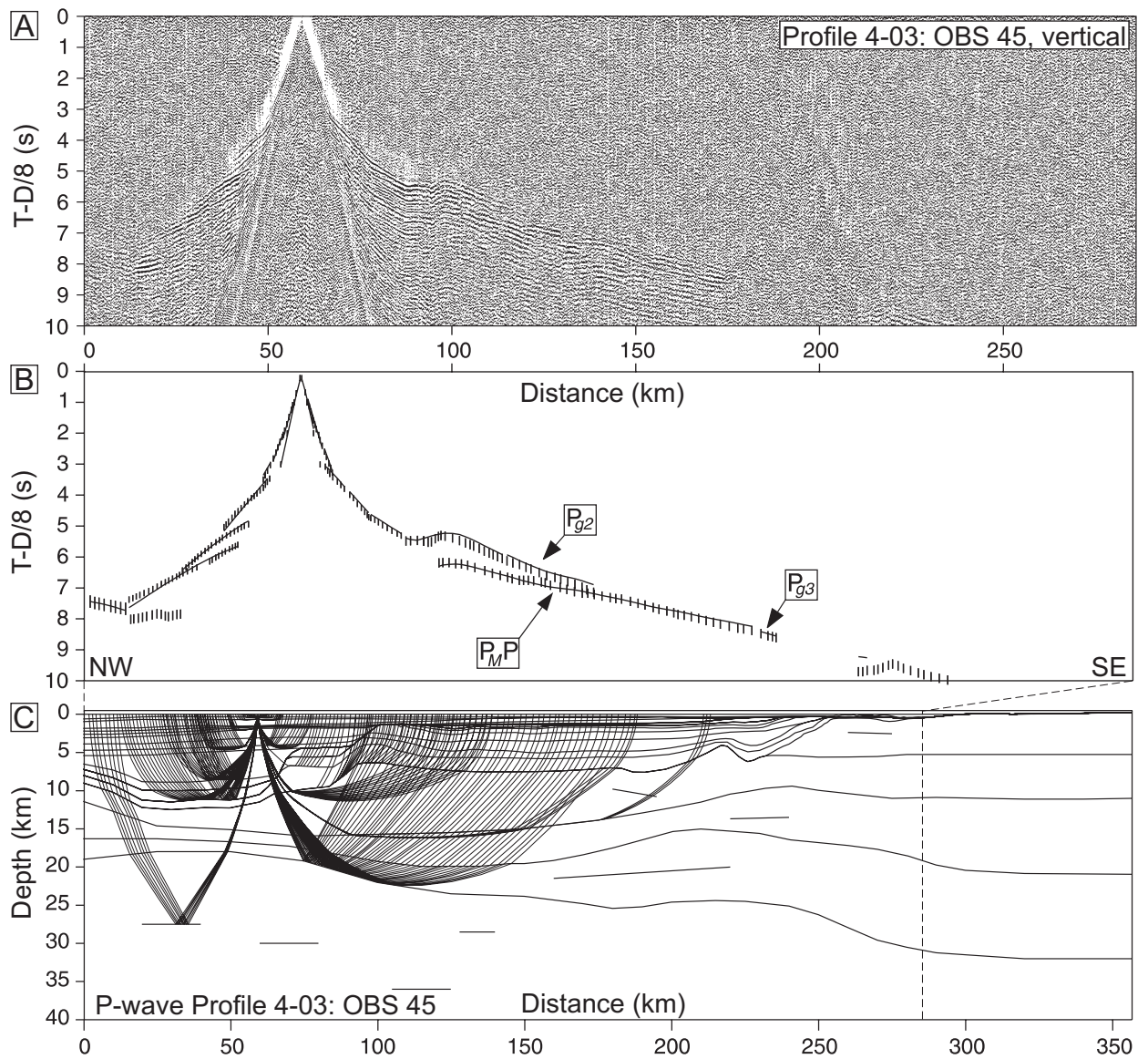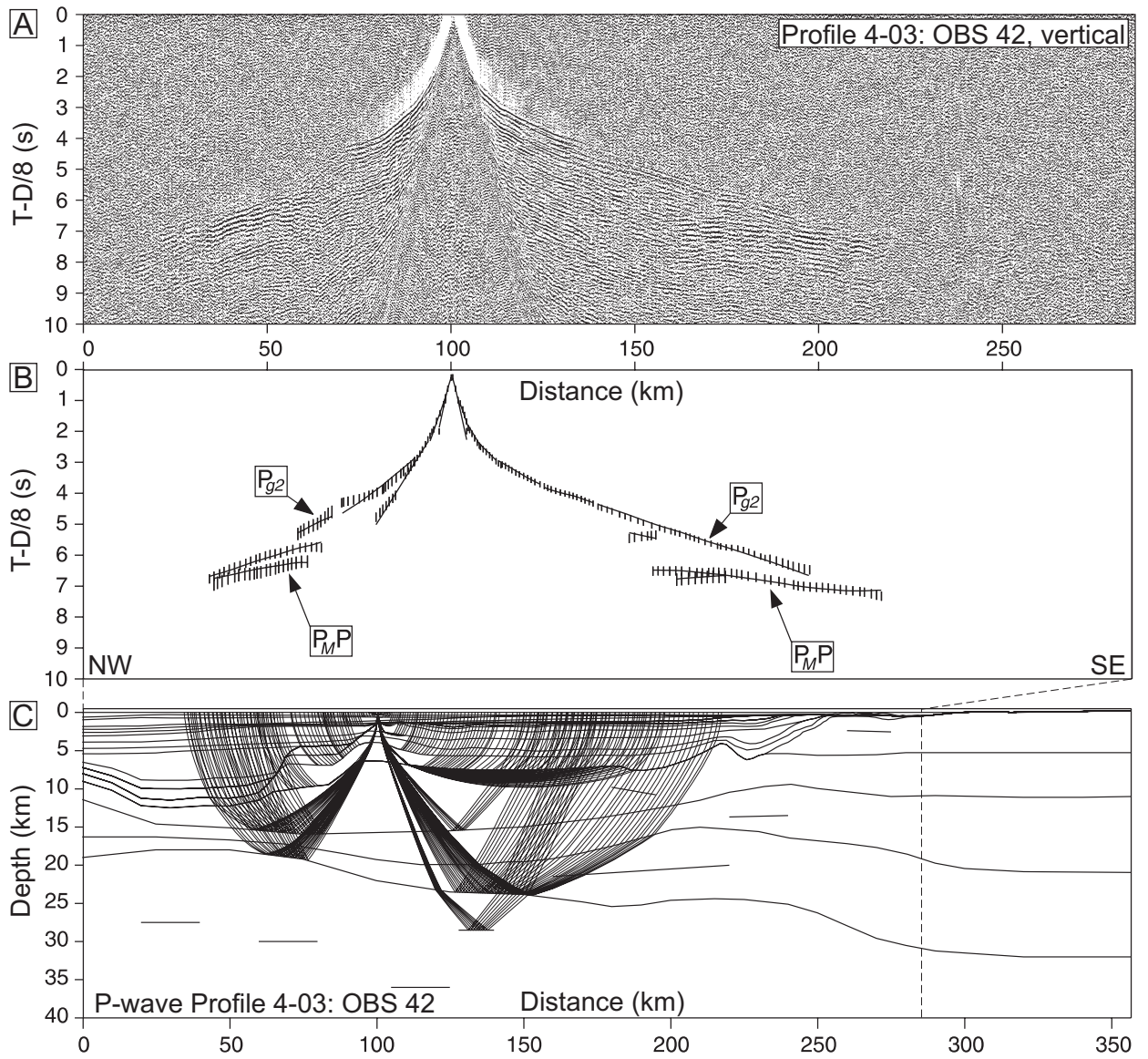

Fig. 3. OBS 46, Profile 4-03. A: OBS data, vertical component. B: Interpretation (vertical bars) and model travel-time (lines) fit. C: Ray-tracing of the velocity model.
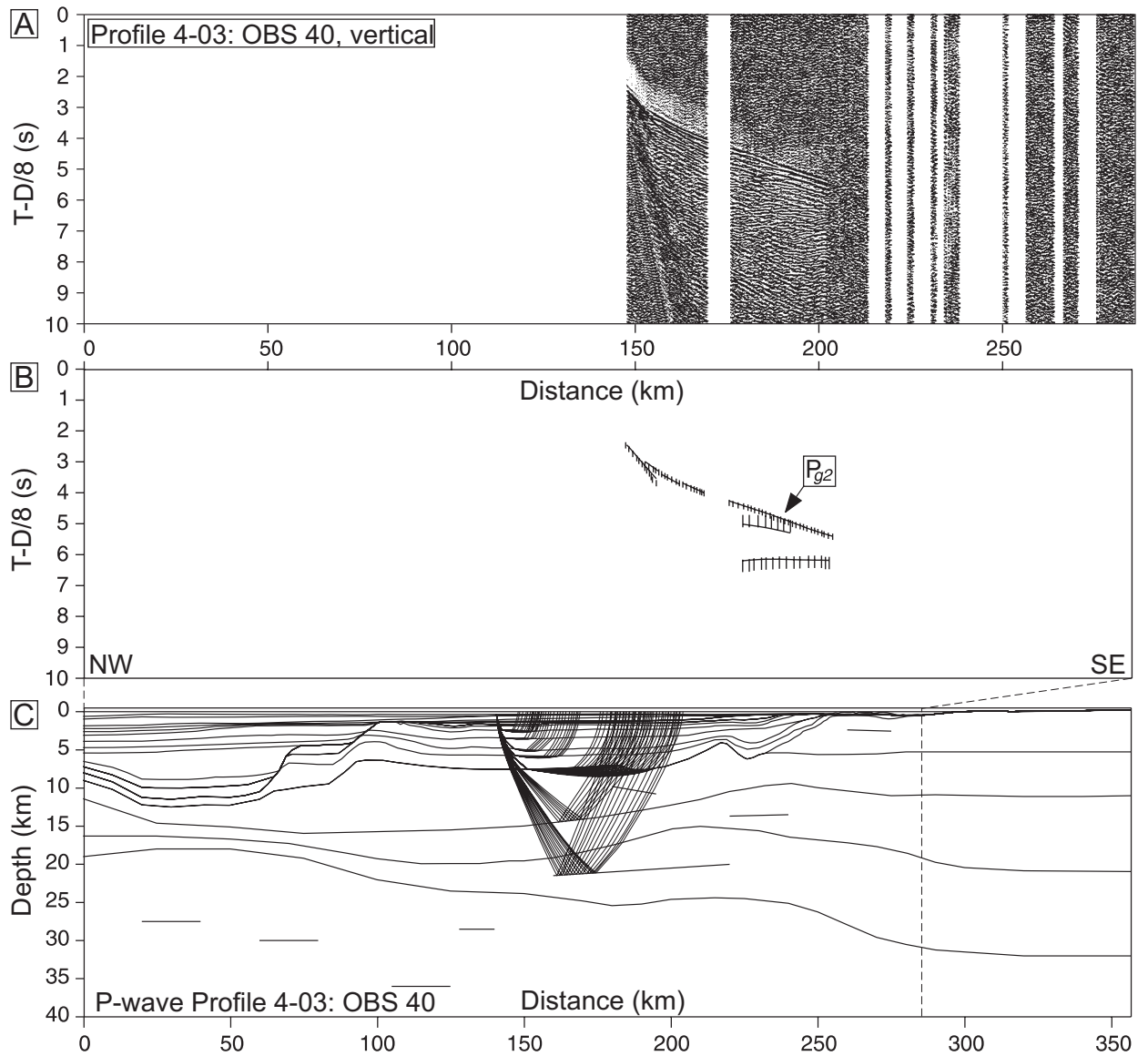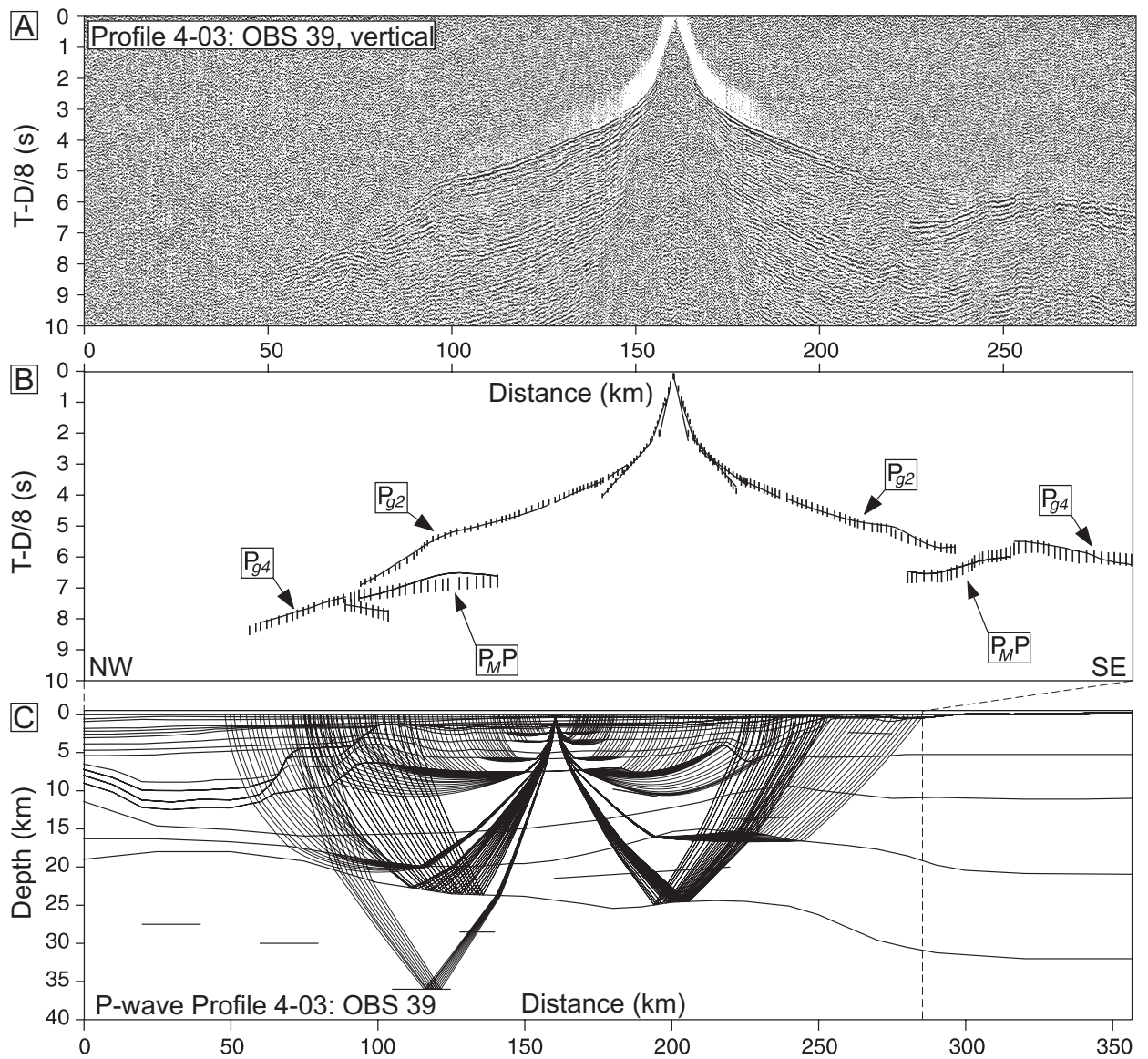
Fig. 4. OBS 45, Profile 4-03. A: OBS data, vertical component. B: Interpretation (vertical bars) and model travel-time (lines) fit. C: Ray-tracing of the velocity model.

Fig. 5. OBS 42, Profile 4-03. A: OBS data, vertical component. B: Interpretation (vertical bars) and model travel-time (lines) fit. C: Ray-tracing of the velocity model.
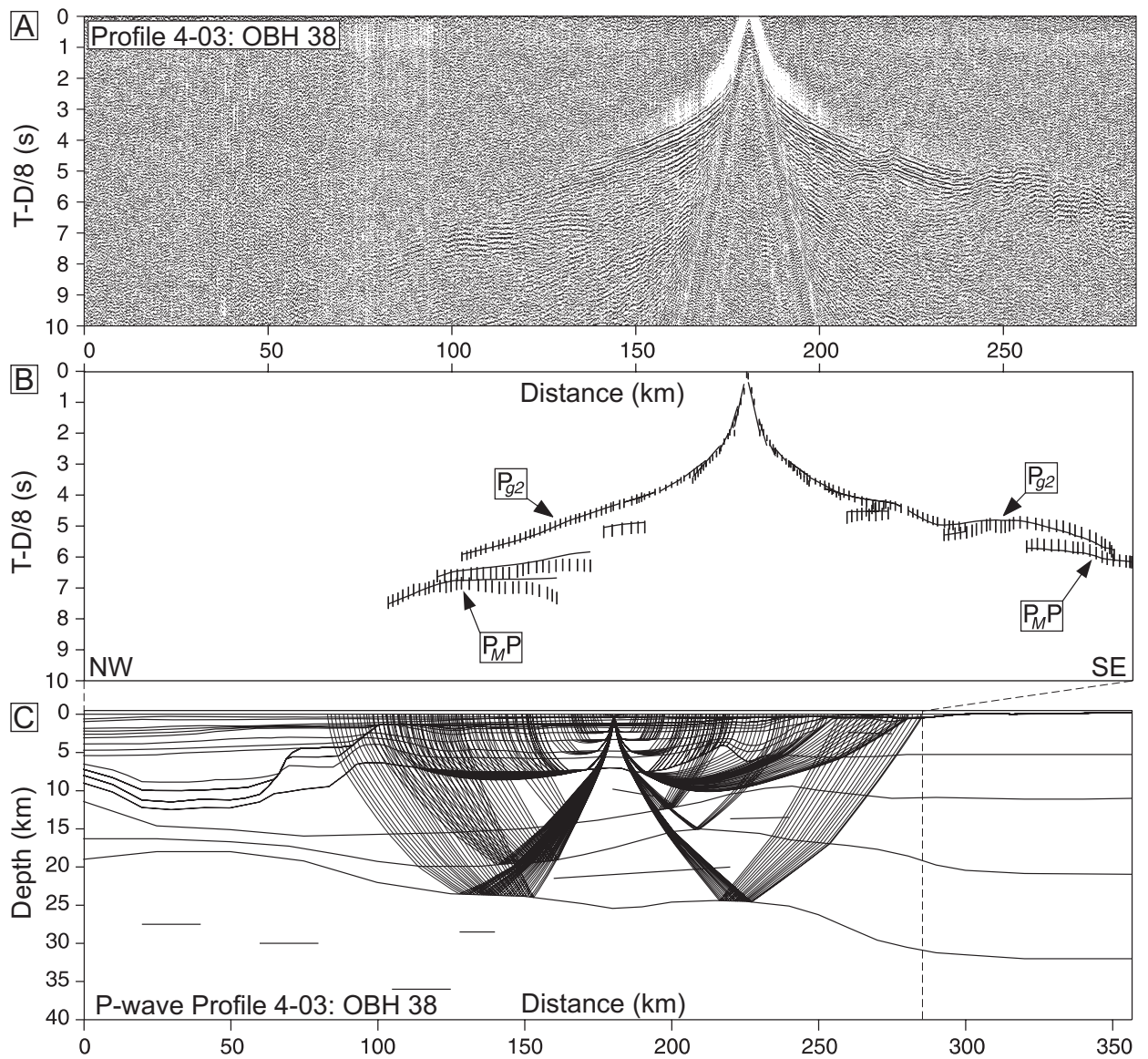
6

Fig. 6. OBS 40, Profile 4-03. A: OBS data, vertical component. Parts of the data were lost due to recording failure. B: Interpretation (vertical bars) and model travel-time (lines) fit. C: Ray-tracing of the velocity model.
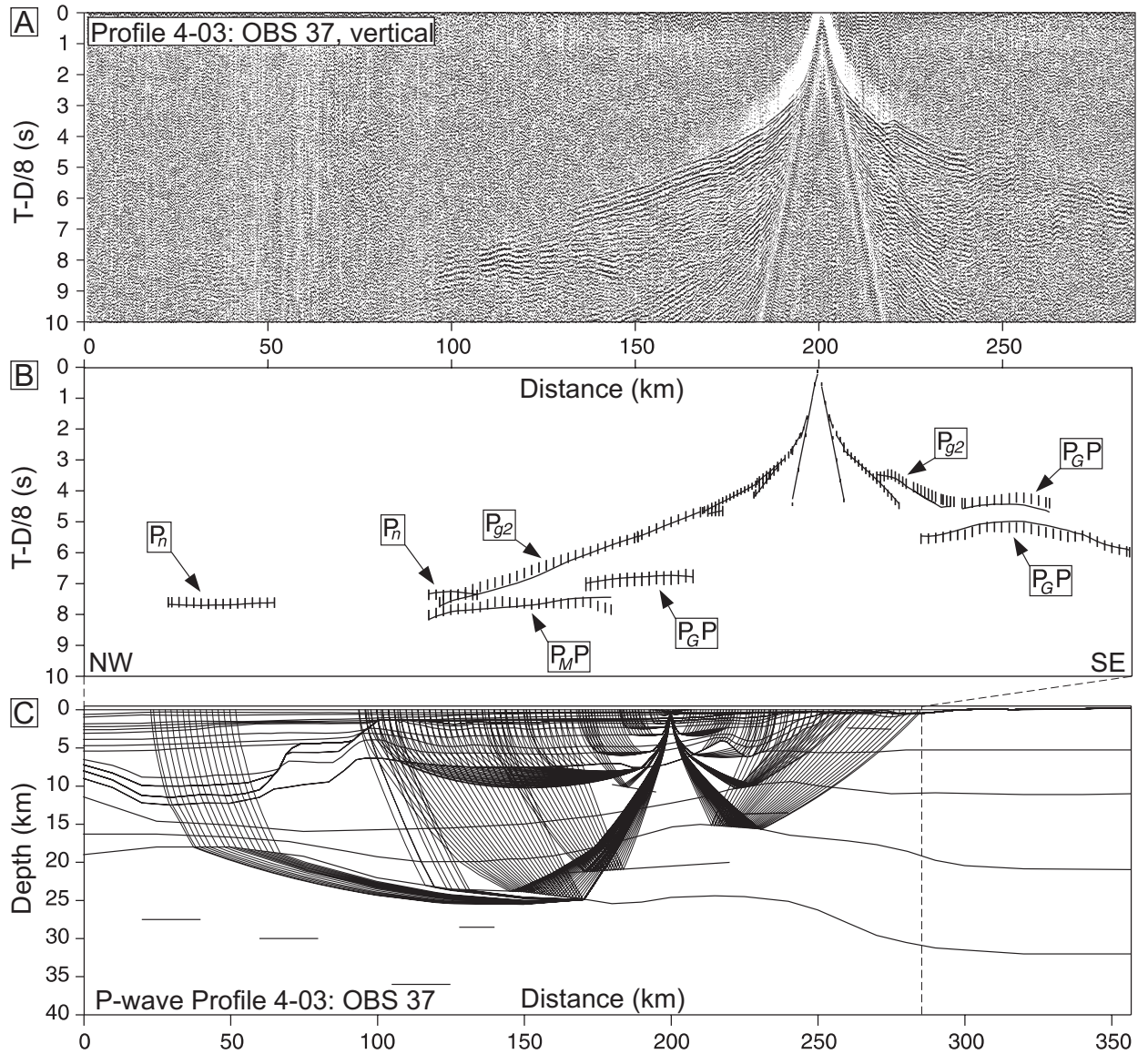
Fig. 7. OBS 39, Profile 4-03. A: OBS data, vertical component. B: Interpretation (vertical bars) and model travel-time (lines) fit. C: Ray-tracing of the velocity model.

8

Fig. 8. OBH 38, Profile 4-03. A: Hydrophone data. B: Interpretation (vertical bars) and model travel-time (lines) fit. C: Ray-tracing of the velocity model.

Fig. 9. OBS 37, Profile 4-03. A: OBS data, vertical component. B: Interpretation (vertical bars) and model travel-time (lines) fit. P_GP: Intra-basement reflections. C: Ray-tracing of the velocity model.
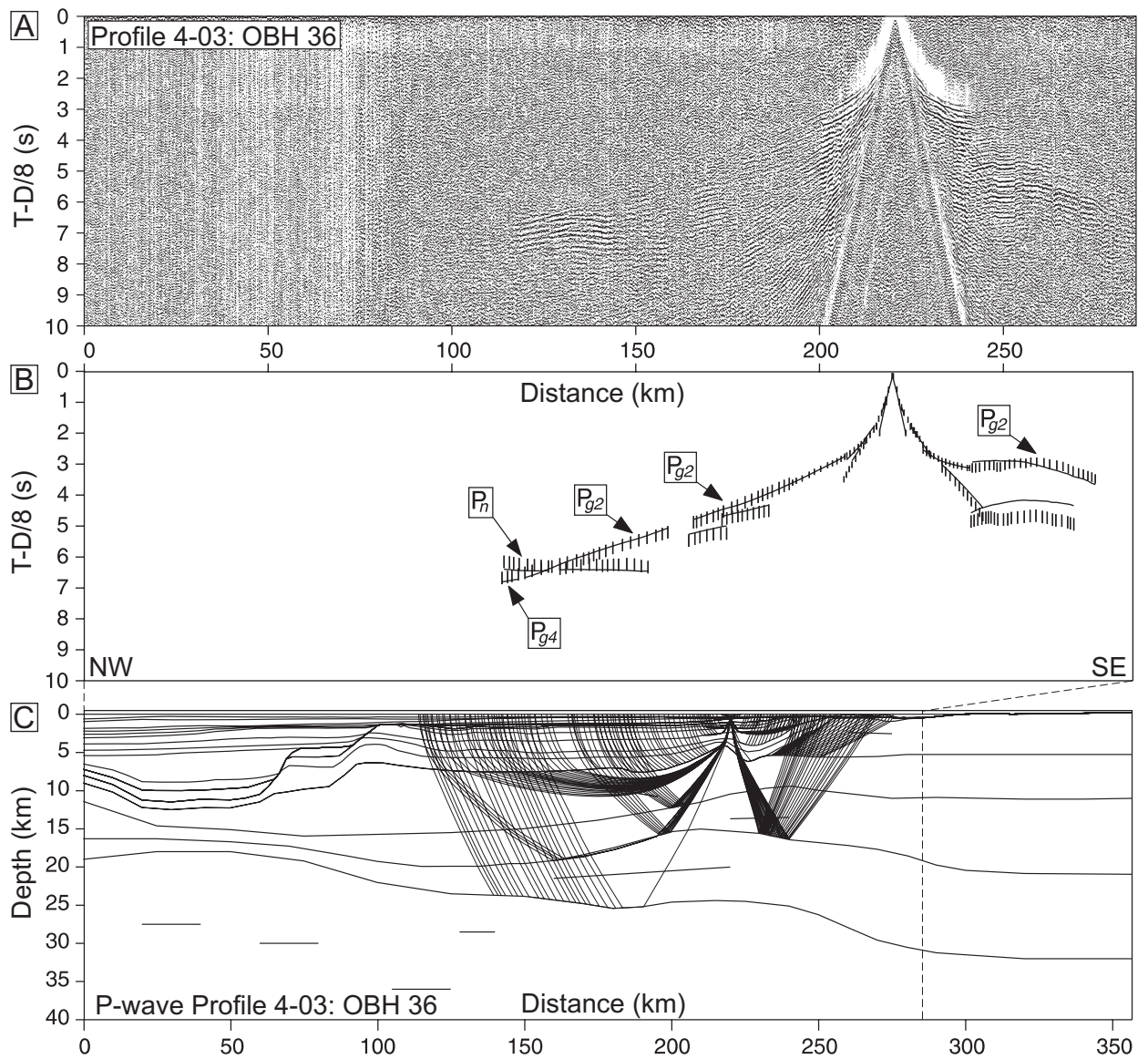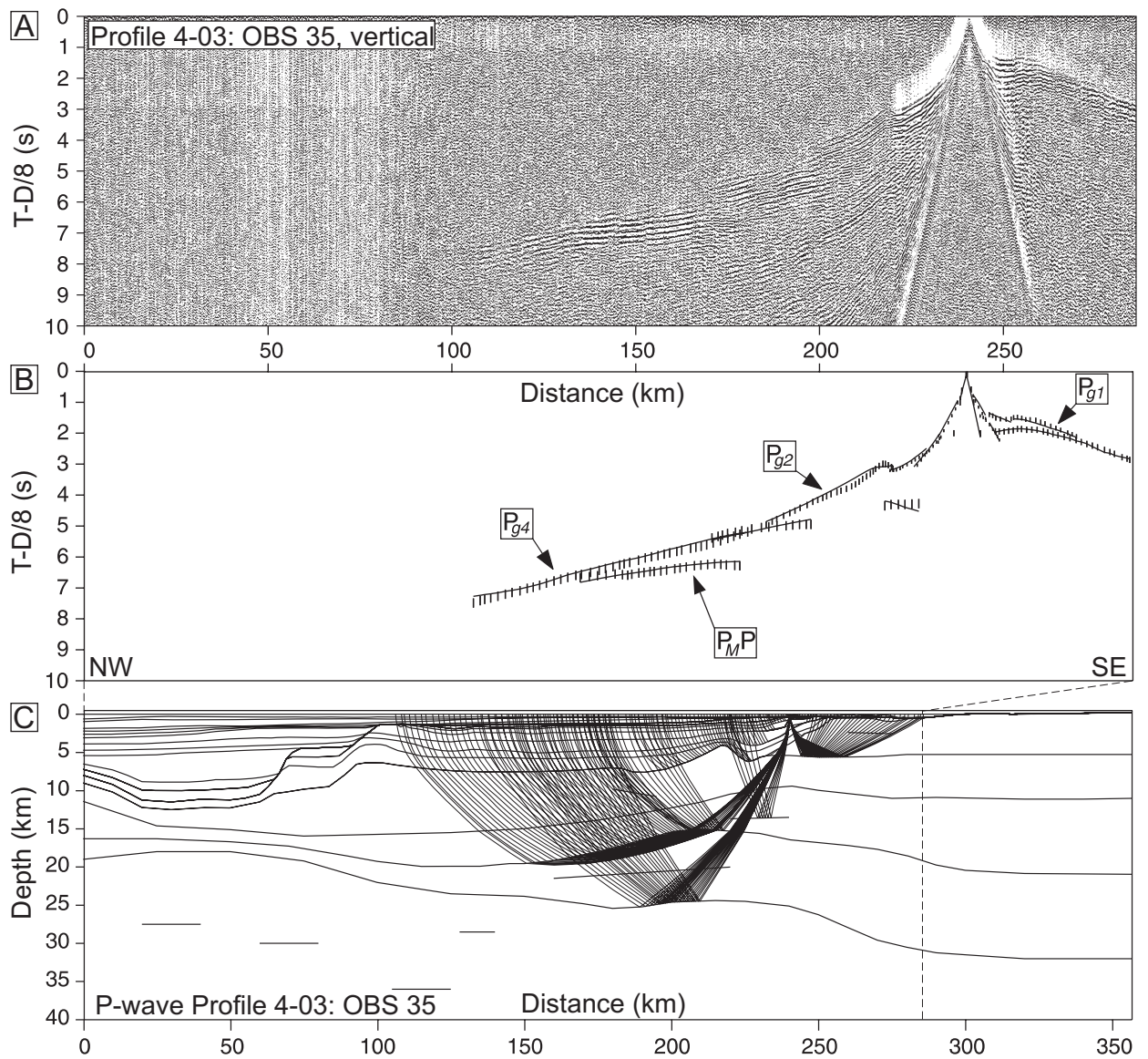
Fig. 10. OBH 36, Profile 4-03. A: Hydrophone data. B: Interpretation (vertical bars) and model travel-time (lines) fit. C: Ray-tracing of the velocity model.

11

Fig. 11. OBS 35, Profile 4-03. A: OBS data, vertical component. B: Interpretation (vertical bars) and model travel-time (lines) fit. C: Ray-tracing of the velocity model.
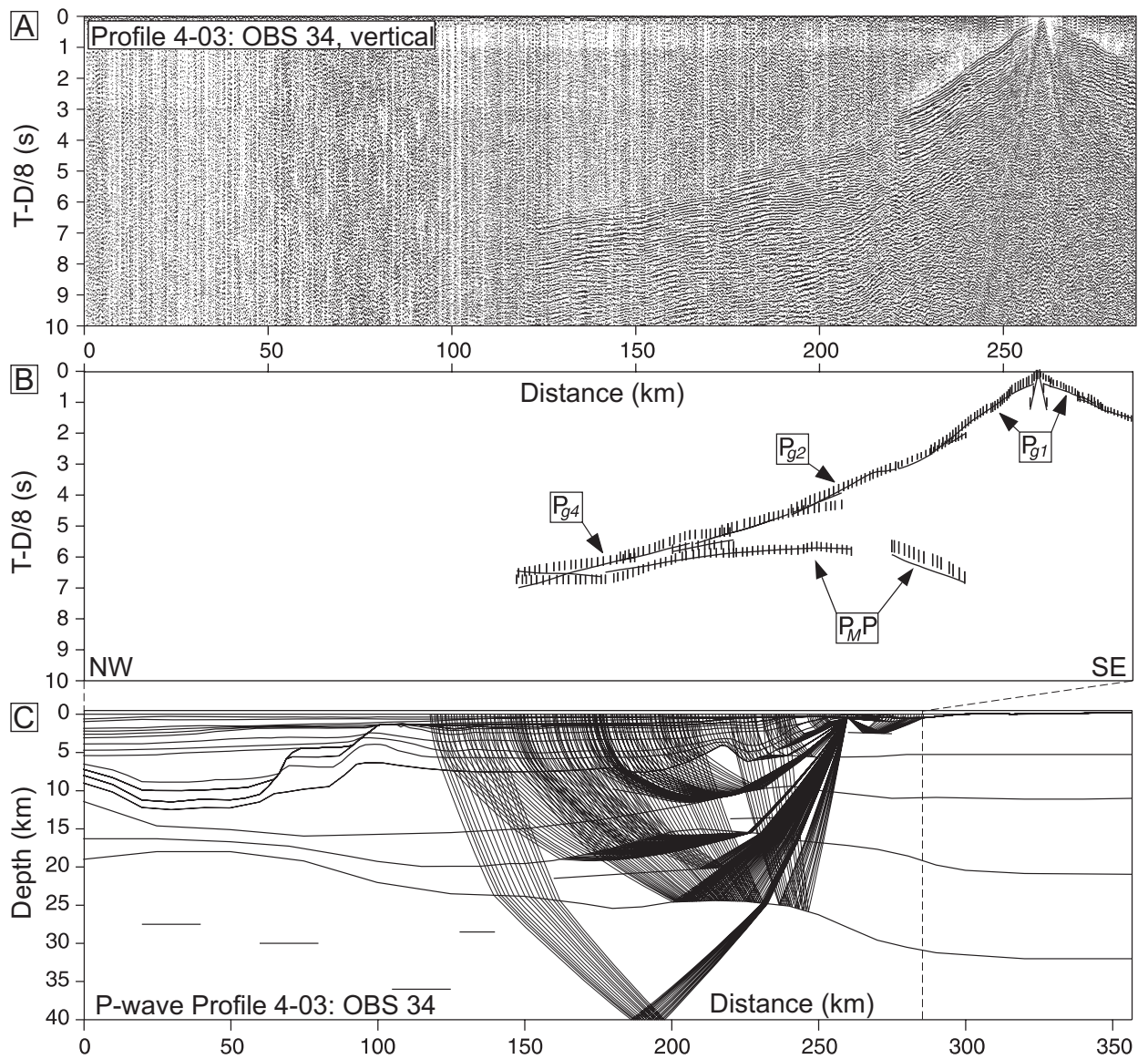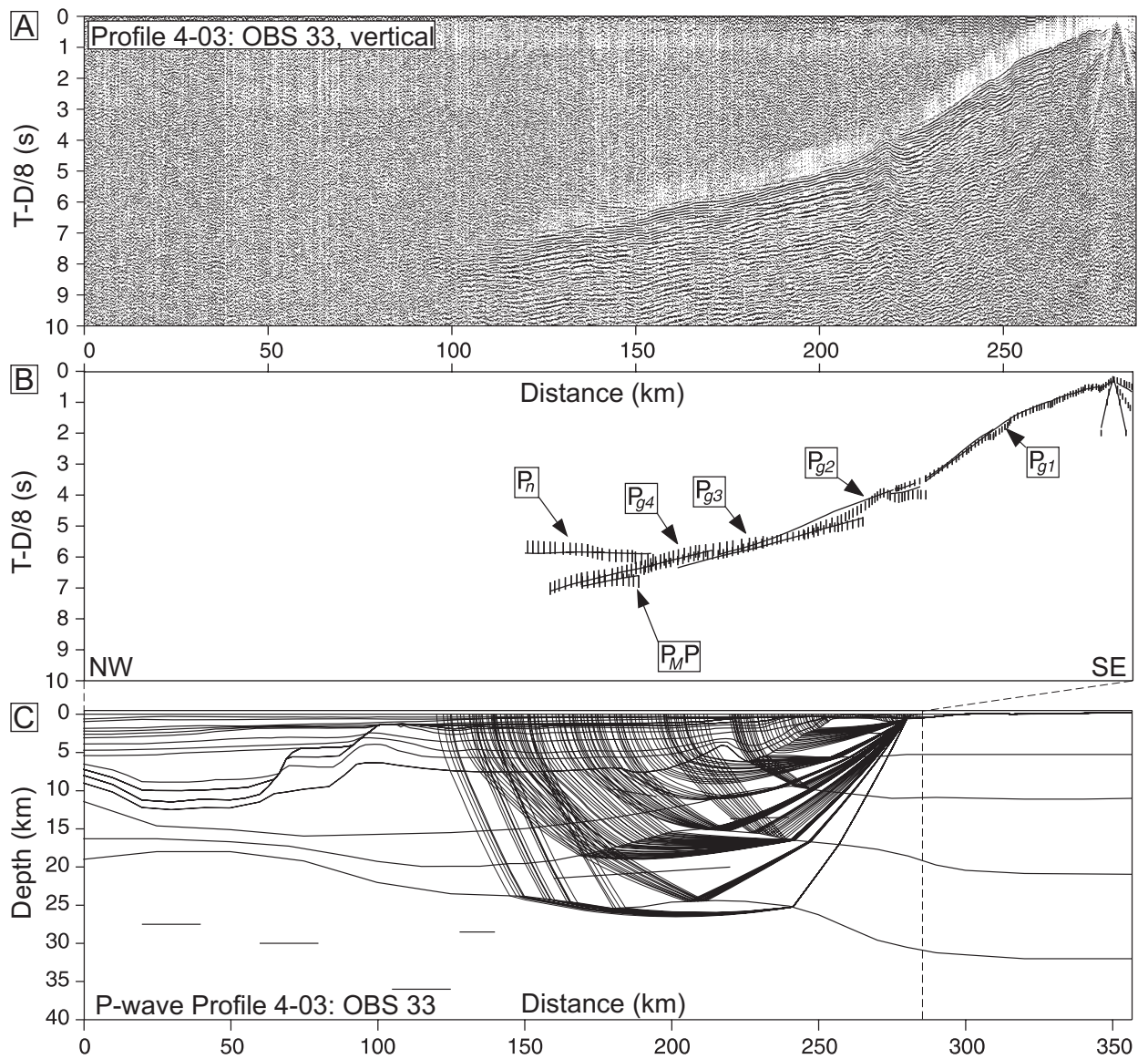
Fig. 12. OBS 34, Profile 4-03. A: OBS data, vertical component. B: Interpretation (vertical bars) and model travel-time (lines) fit. C: Ray-tracing of the velocity model.

Fig. 13. OBS 33, Profile 4-03. A: OBS data, vertical component. B: Interpretation (vertical bars) and model travel-time (lines) fit. C: Ray-tracing of the velocity model.
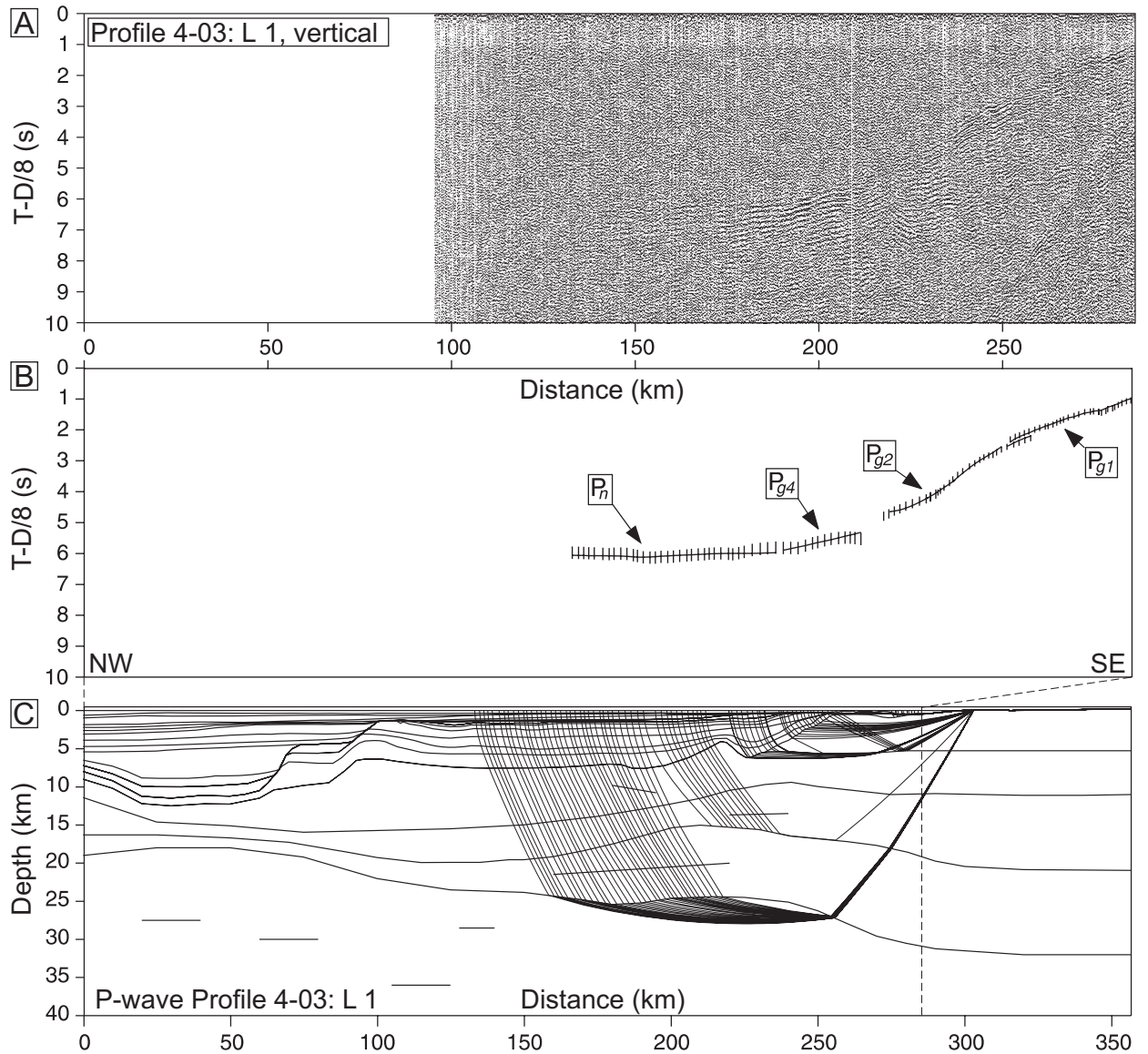
14

Fig. 14. Land station 1, Profile 4-03. A: Seismometer data, vertical component. B: Interpretation (vertical bars) and model travel-time (lines) fit. C: Ray-tracing of the velocity model.
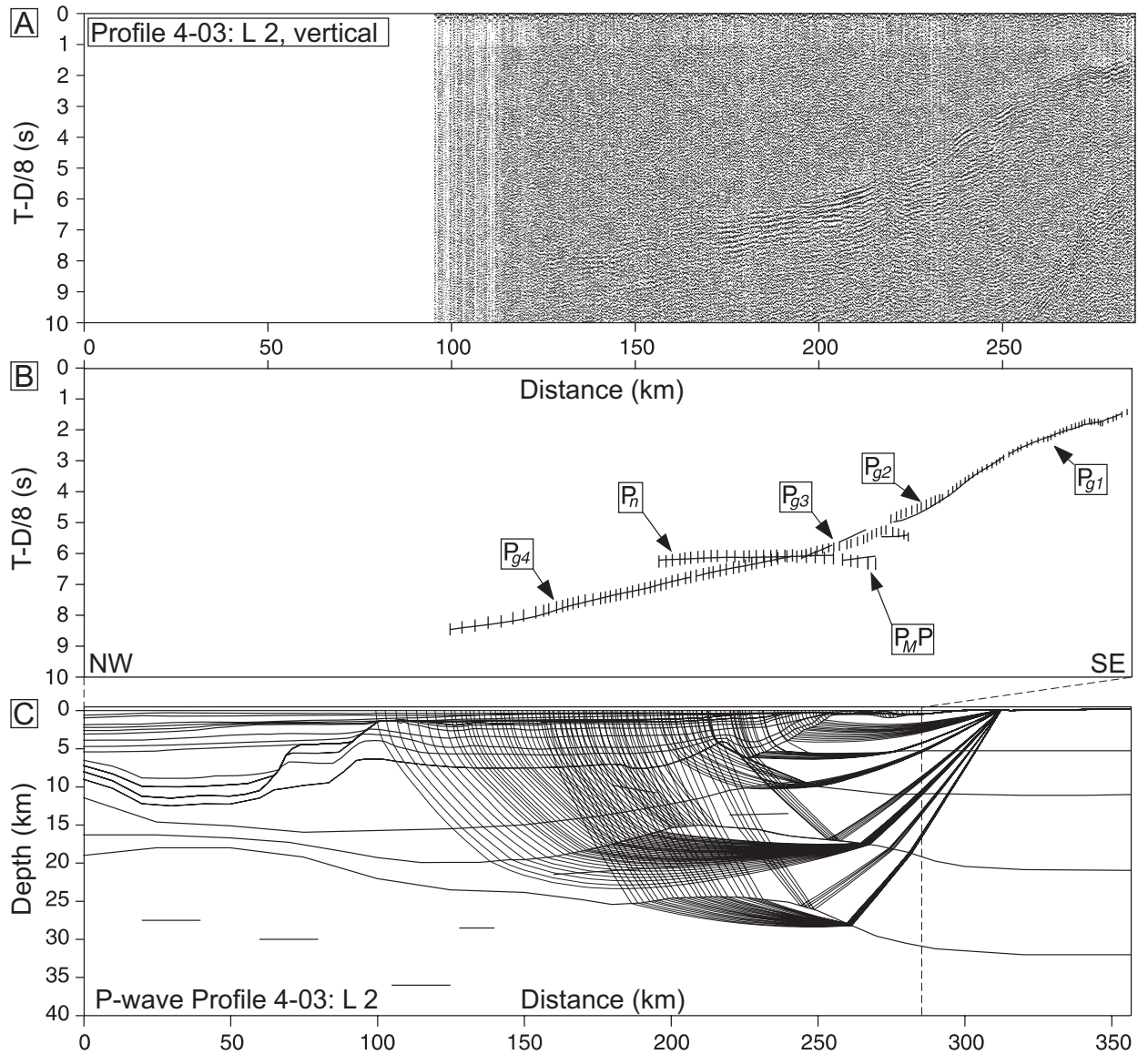
15

Fig. 15. Land station 2, Profile 4-03. A: Seismometer data, vertical component. B: Interpretation (vertical bars) and model travel-time (lines) fit. C: Ray-tracing of the velocity model.
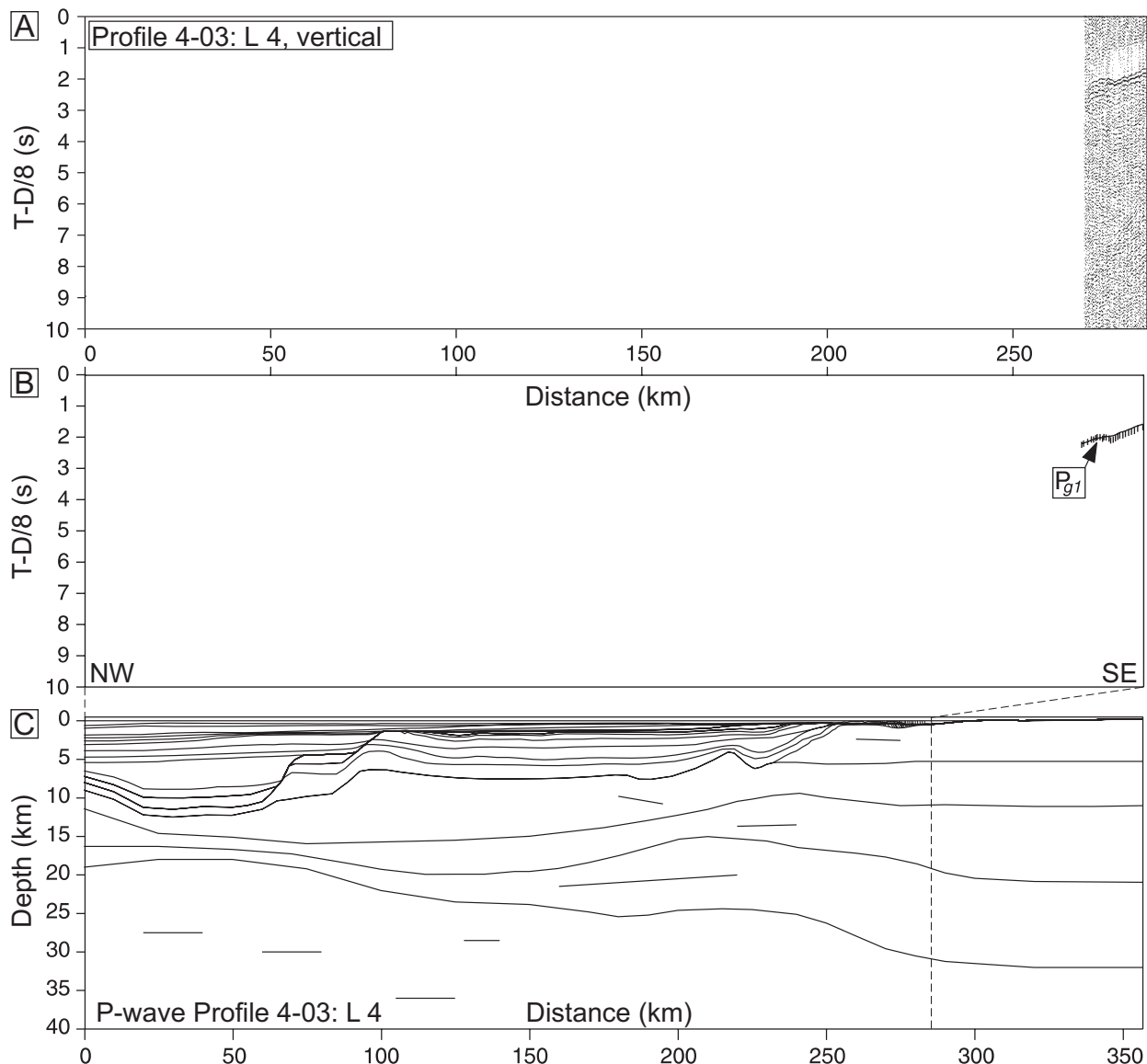
16

Fig. 16. Land station 4, Profile 4-03. A: Seismometer data, vertical component. Much of the data was lost due to recording failure. B: Interpretation (vertical bars) and model travel-time (lines) fit. C: Ray-tracing of the velocity model.

17

A: Profile 4-03: L-5, vertical

T-D/8 (s)

Distance (km)

B: T-D/8 (s)

P_n P_{g4} P_{g2} P_{g1}

NW

SE

C: Depth (km)
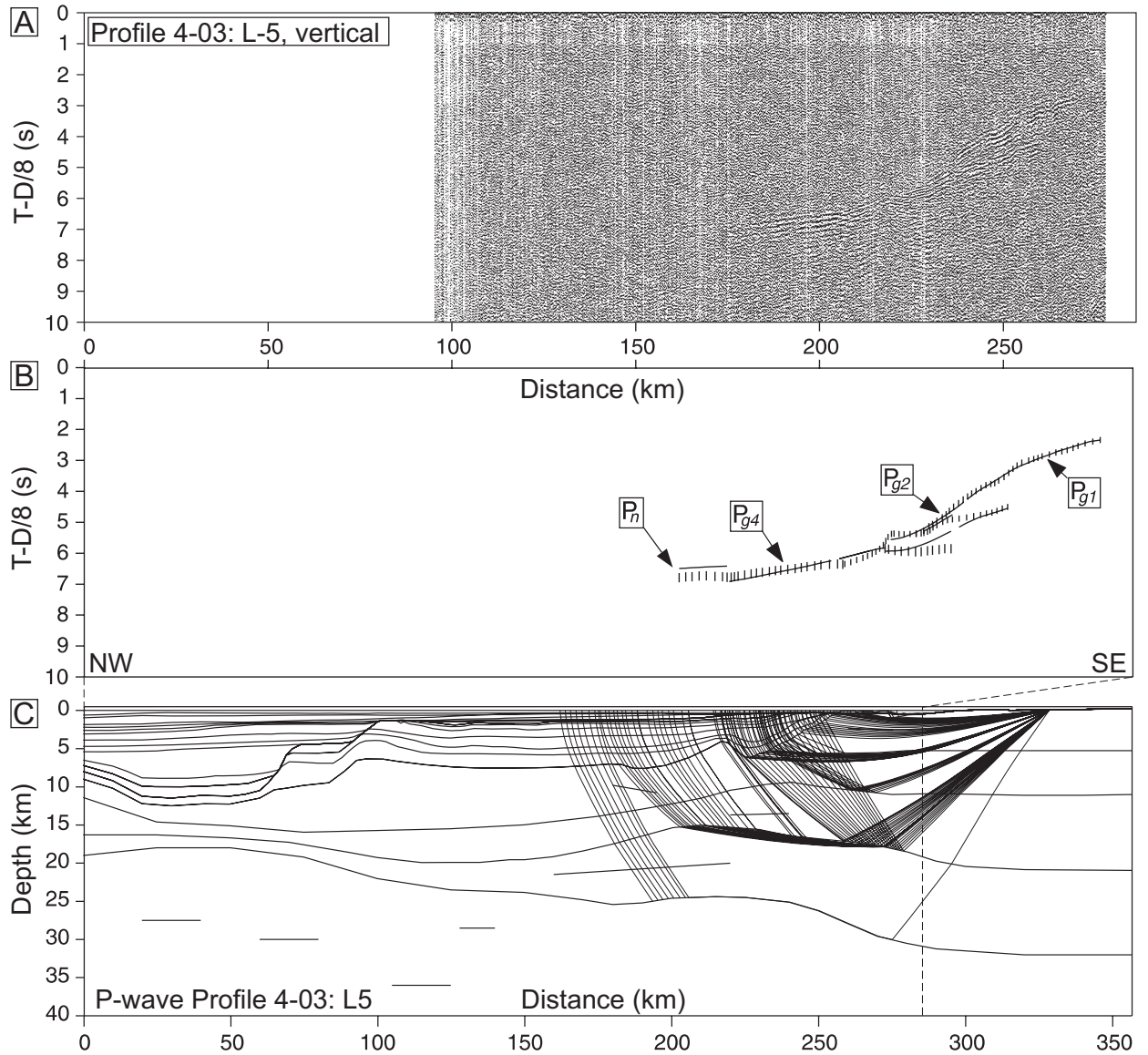
P-wave Profile 4-03: L5 Distance (km)

Fig. 17. Land station 5, Profile 4-03. A: Seismometer data, vertical component. Part of the data near the end of the profile shooting was lost due to recording failure. B: Interpretation (vertical bars) and model travel-time (lines) fit. C: Ray-tracing of the velocity model.
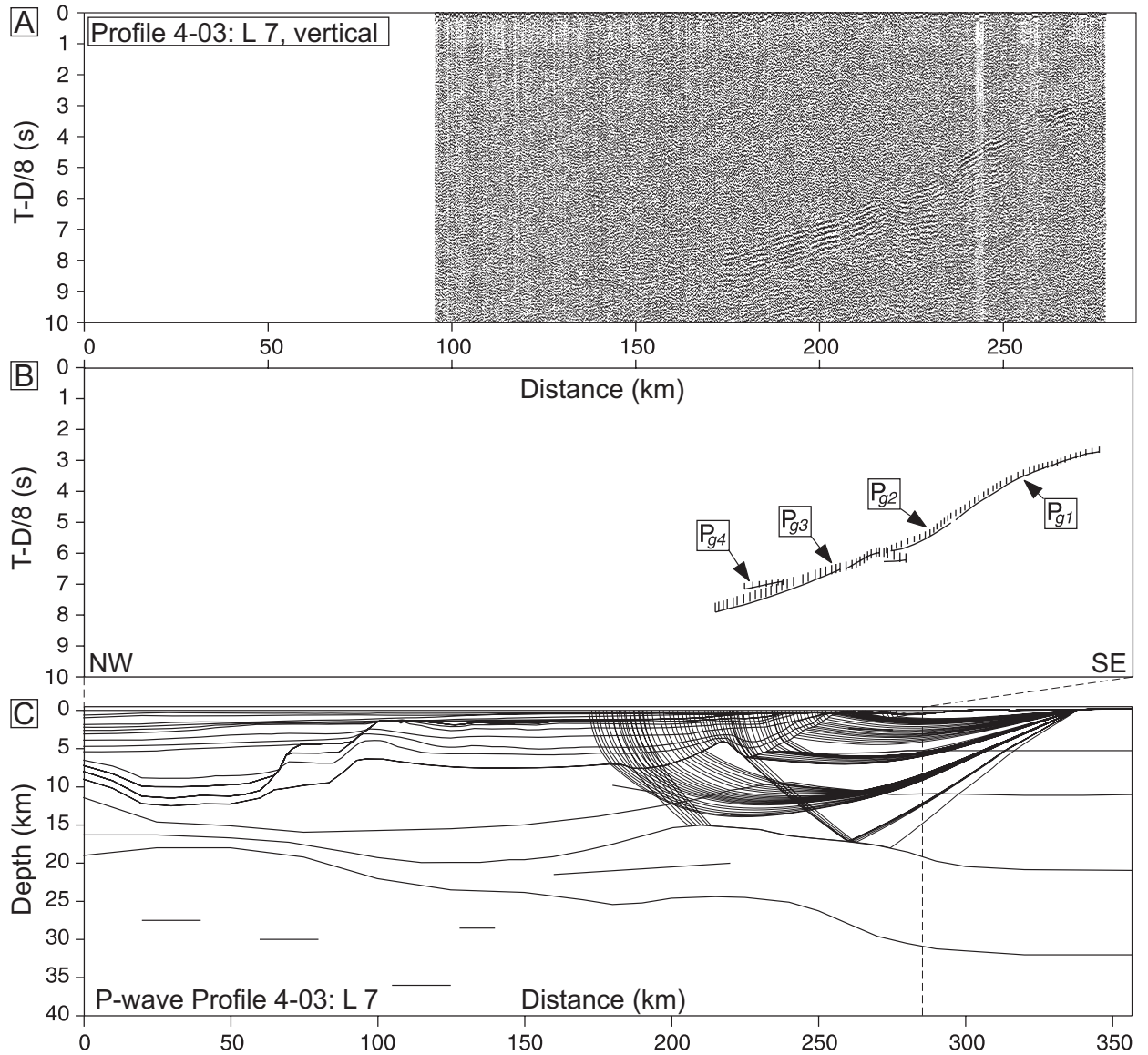
Fig. 18. Land station 7, Profile 4-03. A: Seismometer data, vertical component. Part of the data near the end of the profile shooting was lost due to recording failure. B: Interpretation (vertical bars) and model travel-time (lines) fit. C: Ray-tracing of the velocity model.
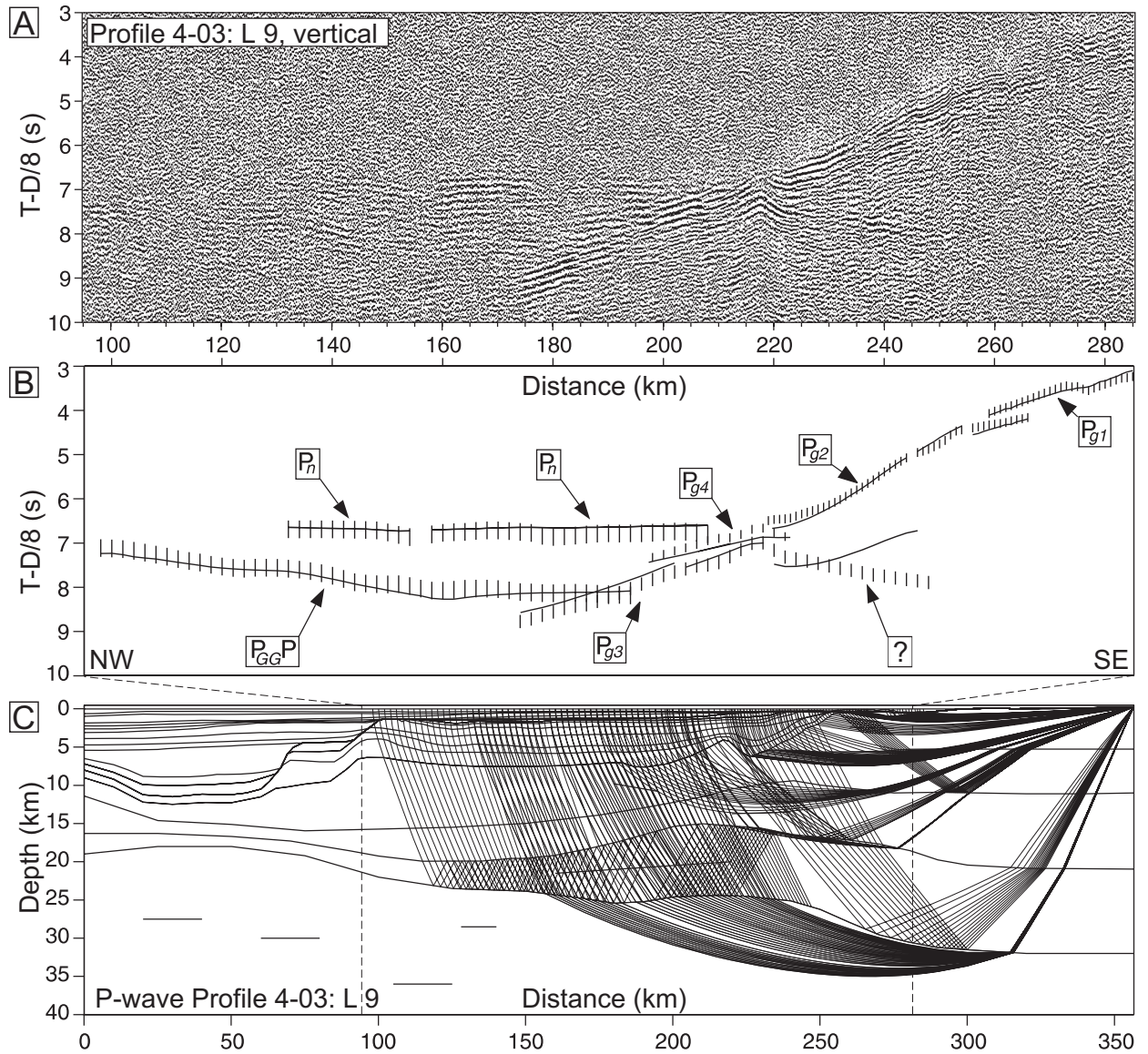
19

Fig. 19. Land station 9, Profile 4-03. A: Seismometer data, vertical component. B: Interpretation (vertical bars) and model travel-time (lines) fit. $P_{GG}P$: Lower-basement peg-leg reflection. C: Ray-tracing of the velocity model.
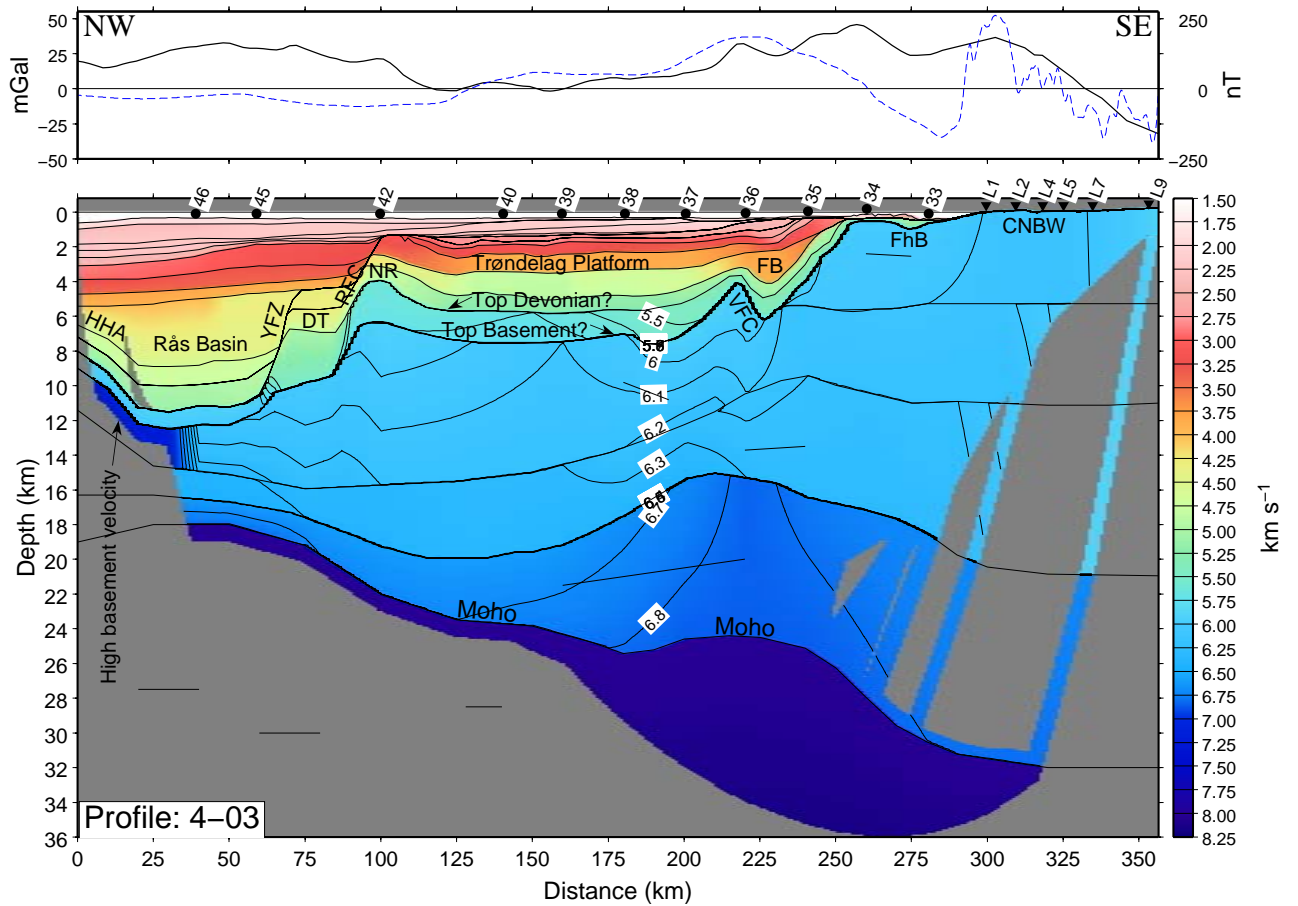
20

Fig. 20. Upper panel: Observed gravity (heavy line) and magnetic anomalies (dashed blue line) along Profile 4-03. Lower panel: Gridded crustal velocity model of Profile 4-03. The parts of the model not covered by rays are masked. Floating reflectors are not included in the ray-coverage. Contour interval within the basement is 0.1 km s^{-1}. CNBW: Central Norway Basement Window, DT: Dønna Terrace, FB: Froan Basin, FhB: Frohavet Basin, HHA: Helland-Hansen Arch, RFC: Revfallet Fault Complex, VFC: Vingleia Fault Complex, YFZ: Ytreholmen Fault Zone.

Profile 3-03

The profile has data from 12 OBS/Hs and 5 land seismometers (Figs. 21-37). These are OBS/Hs 21-32, and land stations 2, 3, 6, 8, 10. Data and models are presented from NW to SE, starting with OBS 32. The velocity model used for the ray tracing is shown in Fig. 38.
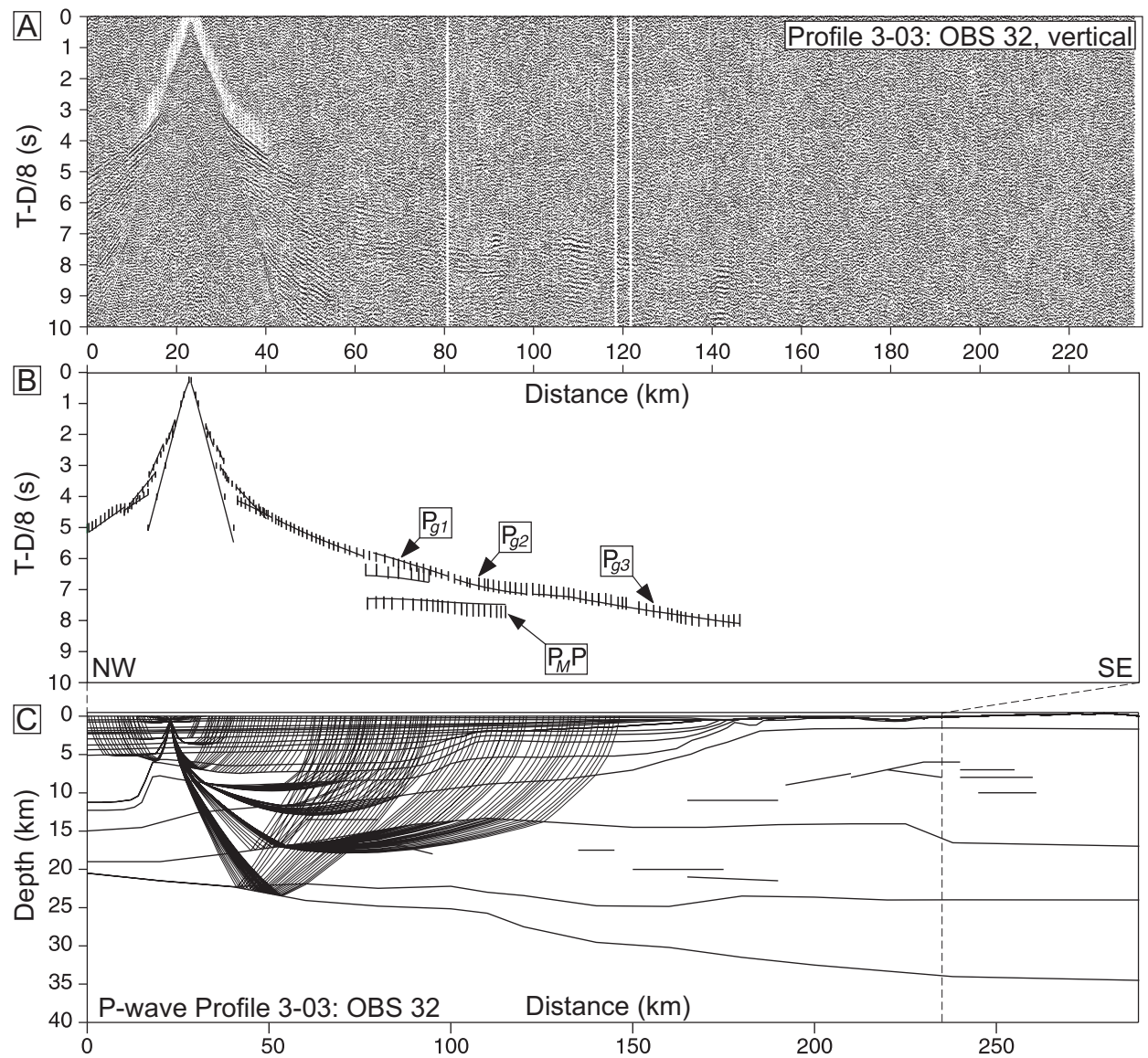

Fig. 21. OBS 32, Profile 3-03. A: OBS data, vertical component. B: Interpretation (vertical bars) and model travel-time (lines) fit. C: Ray-tracing of the velocity model.
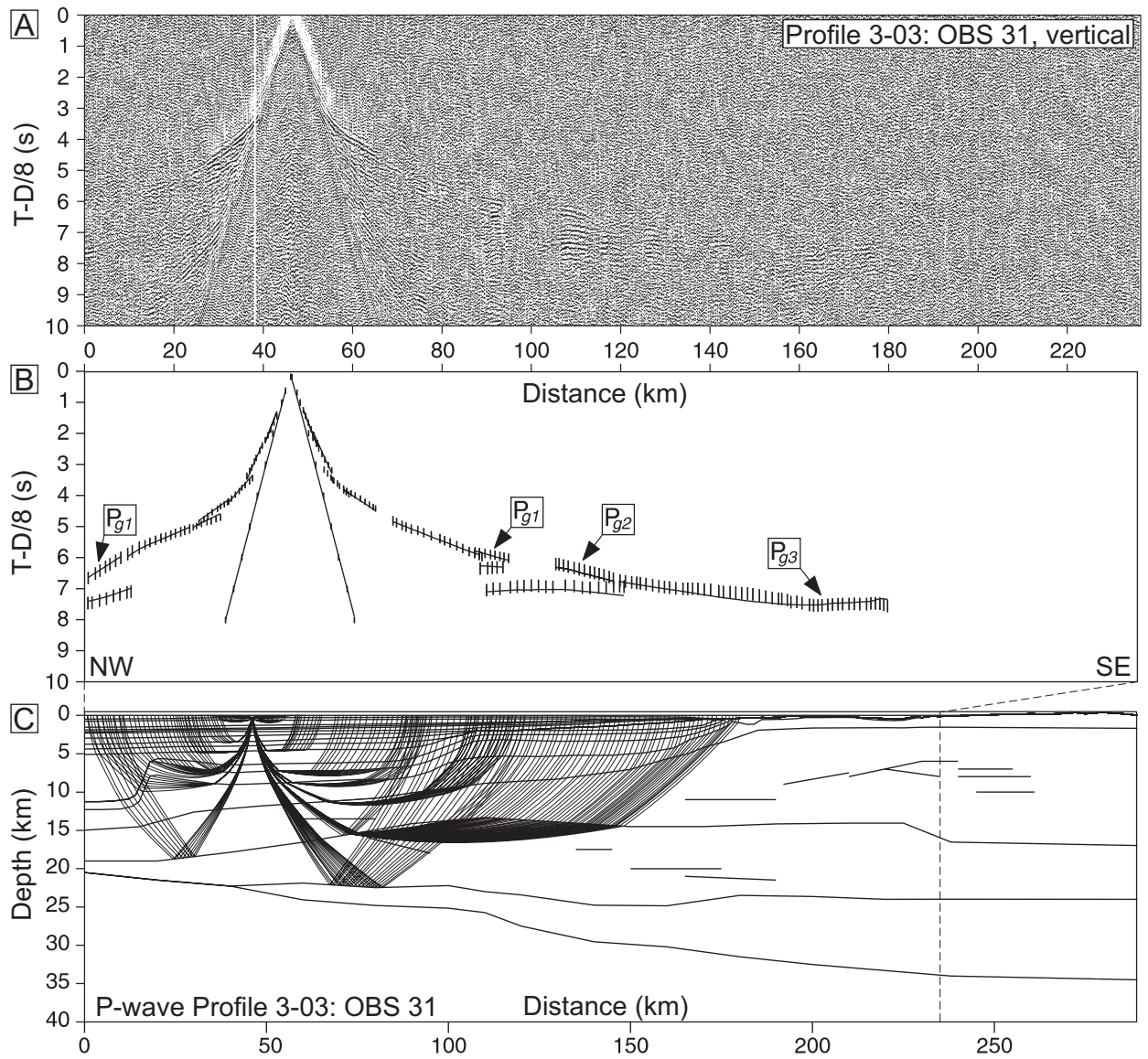
Fig. 22. OBS 31, Profile 3-03. A: OBS data, vertical component. B: Interpretation (vertical bars) and model travel-time (lines) fit. C: Ray-tracing of the velocity model.
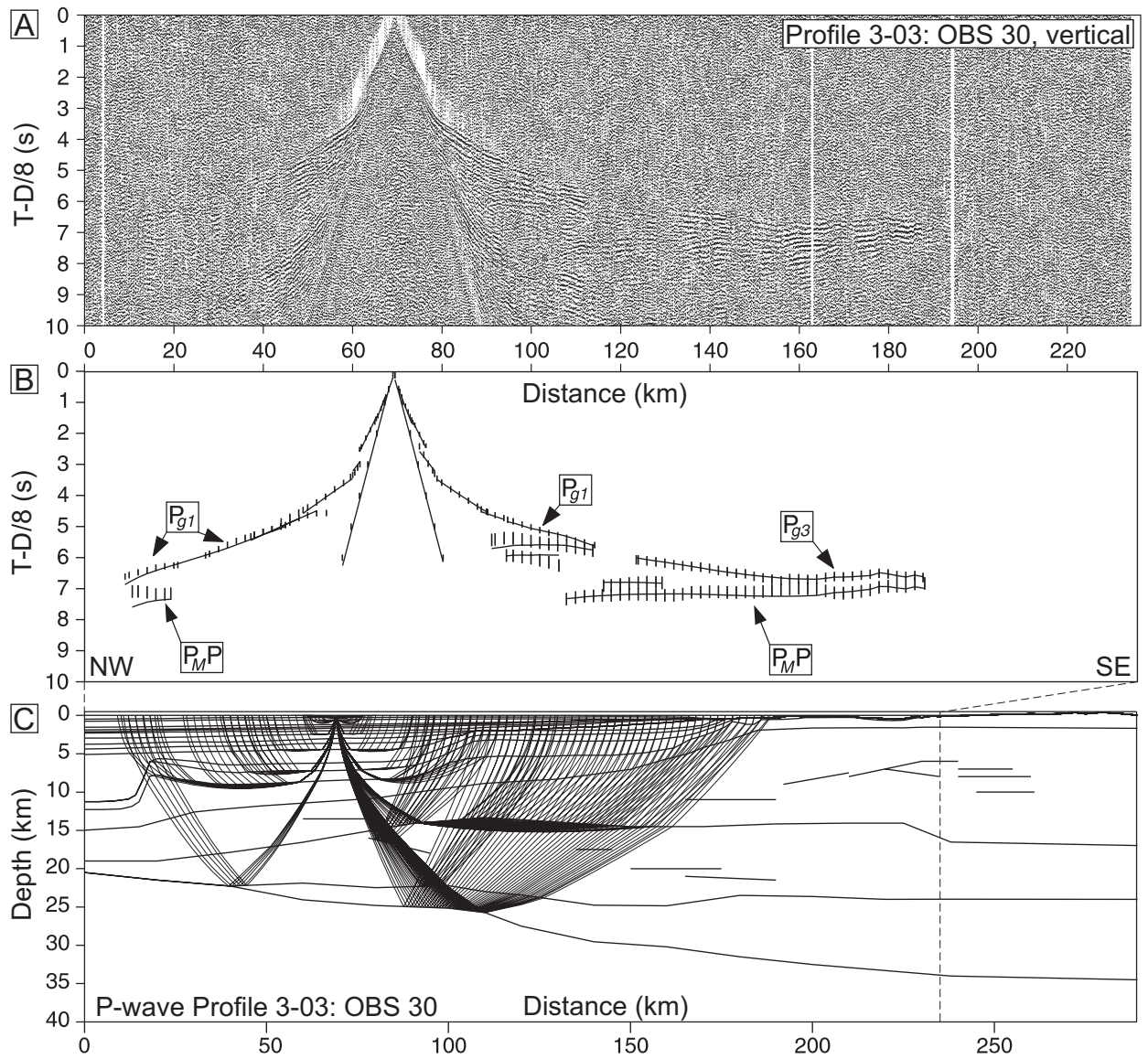
23

Fig. 23. OBS 30, Profile 3-03. A: OBS data, vertical component. B: Interpretation (vertical bars) and model travel-time (lines) fit. C: Ray-tracing of the velocity model.
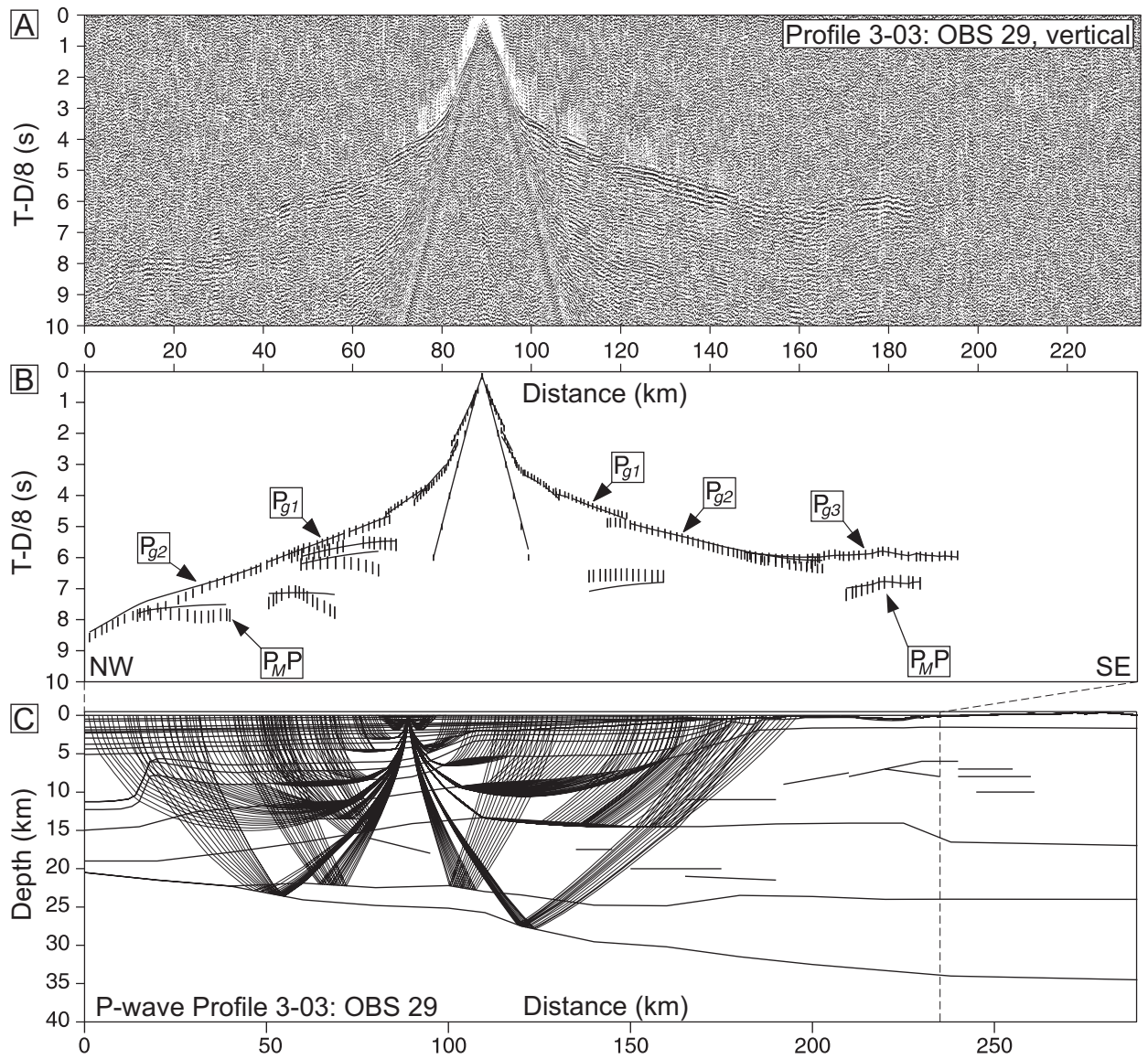
Fig. 24. OBS 29, Profile 3-03. A: OBS data, vertical component. B: Interpretation (vertical bars) and model travel-time (lines) fit. C: Ray-tracing of the velocity model.
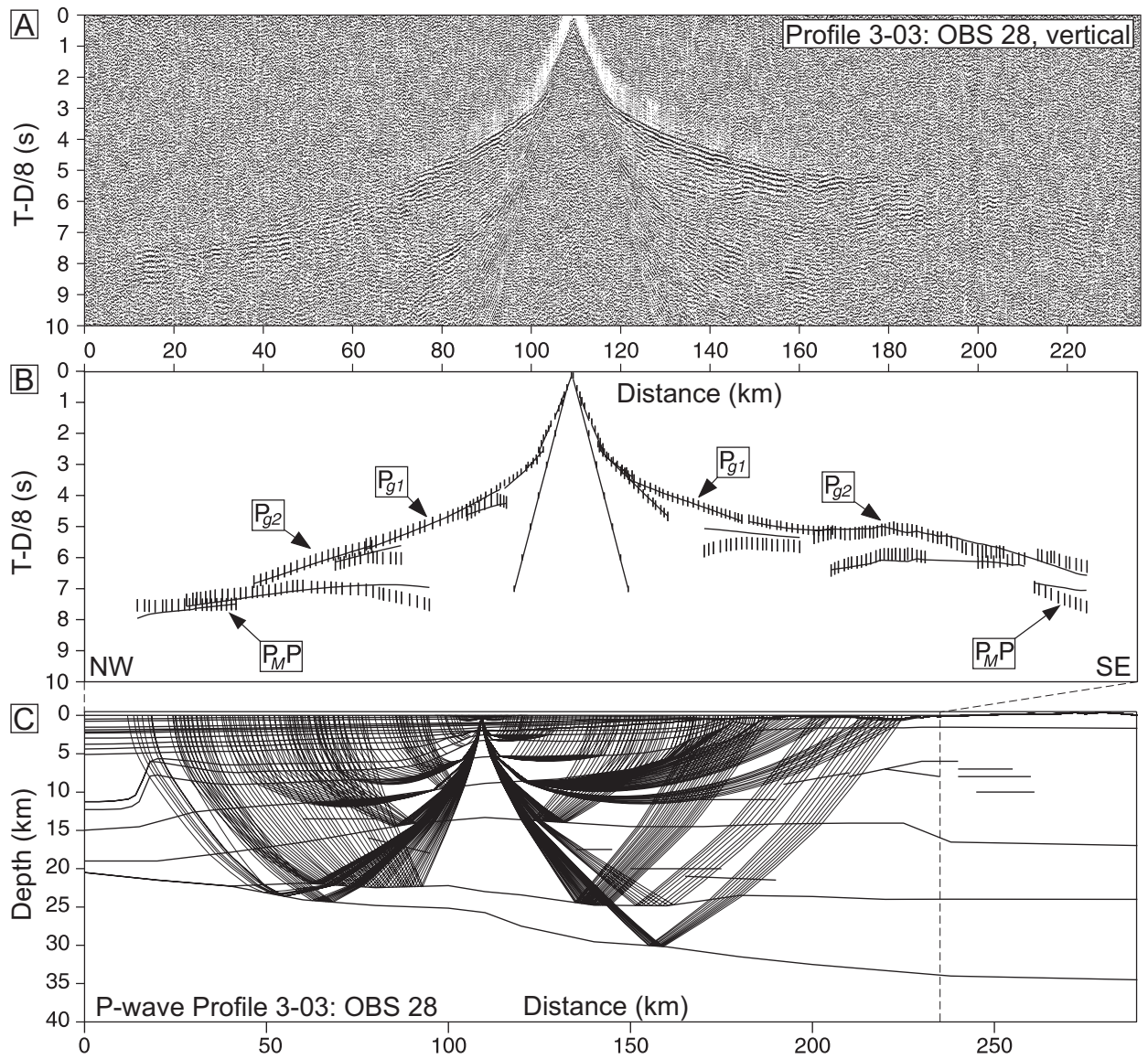
Fig. 25. OBS 28, Profile 3-03. A: OBS data, vertical component. B: Interpretation (vertical bars) and model travel-time (lines) fit. C: Ray-tracing of the velocity model.
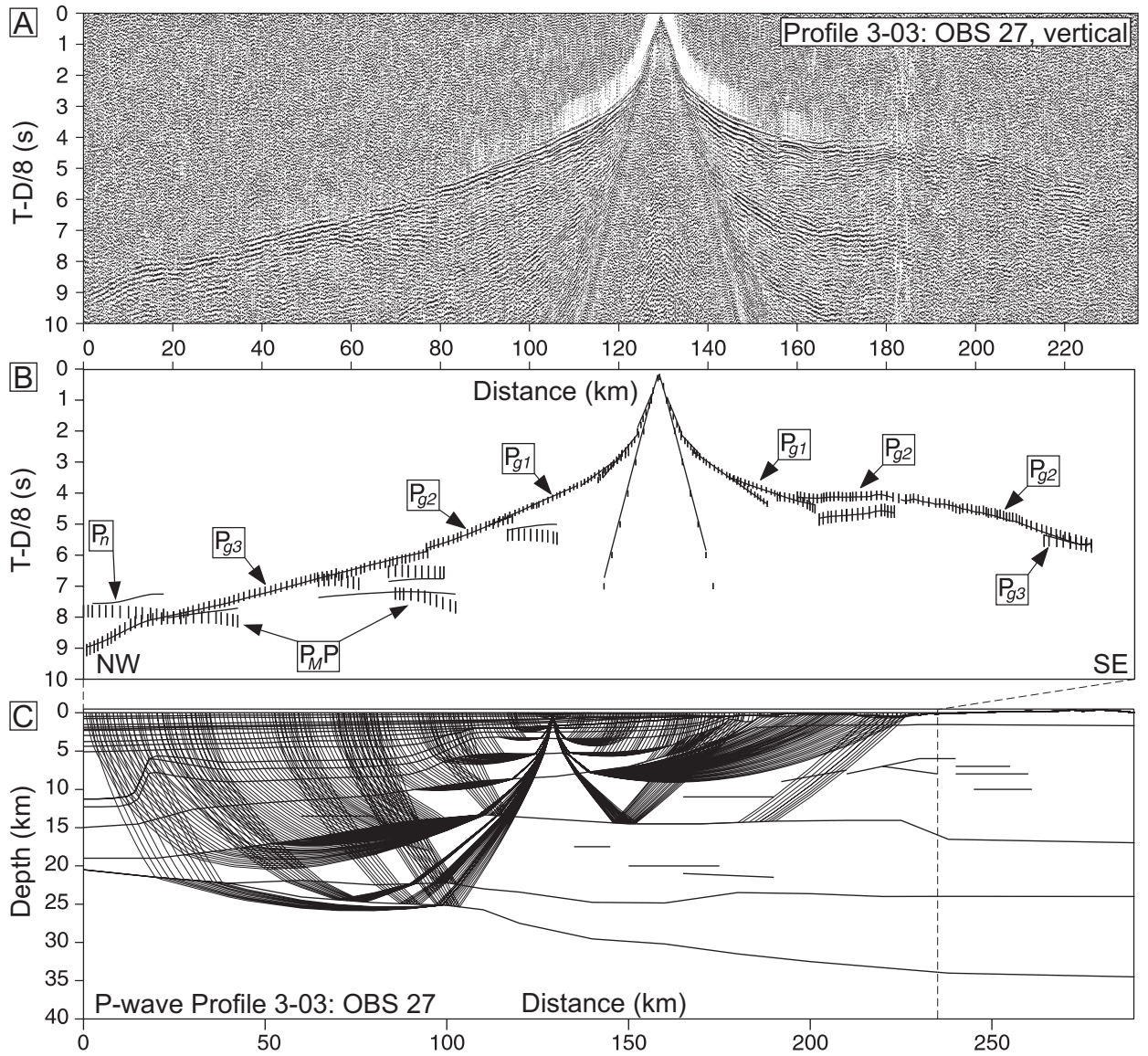
26

Fig. 26. OBS 27, Profile 3-03. A: OBS data, vertical component. B: Interpretation (vertical bars) and model travel-time (lines) fit. C: Ray-tracing of the velocity model.
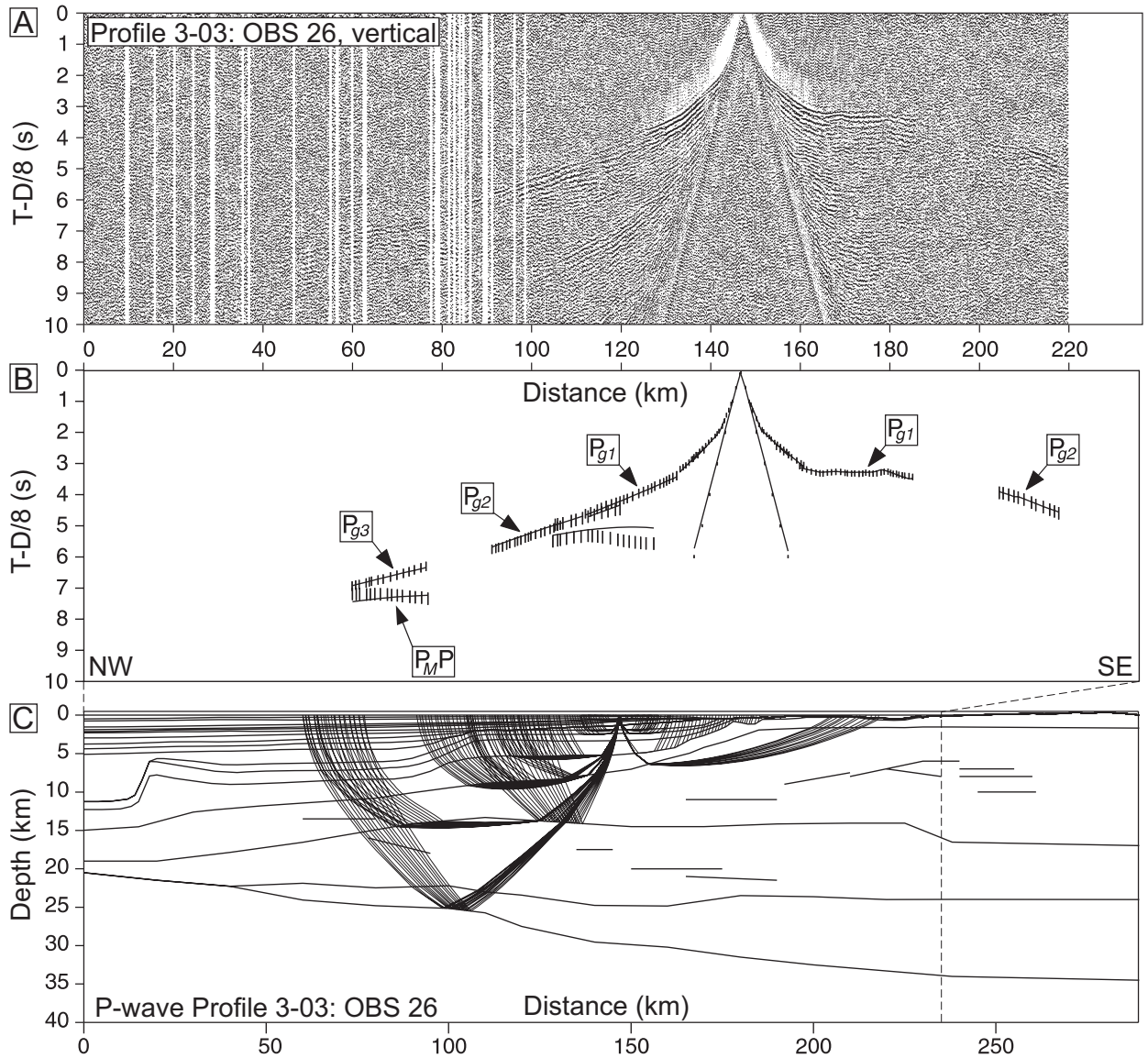
Fig. 27. OBS 26, Profile 3-03. A: OBS data, vertical component. Part of the data along and near the end of the profile shooting was lost due to recording failure. B: Interpretation (vertical bars) and model travel-time (lines) fit. C: Ray-tracing of the velocity model.
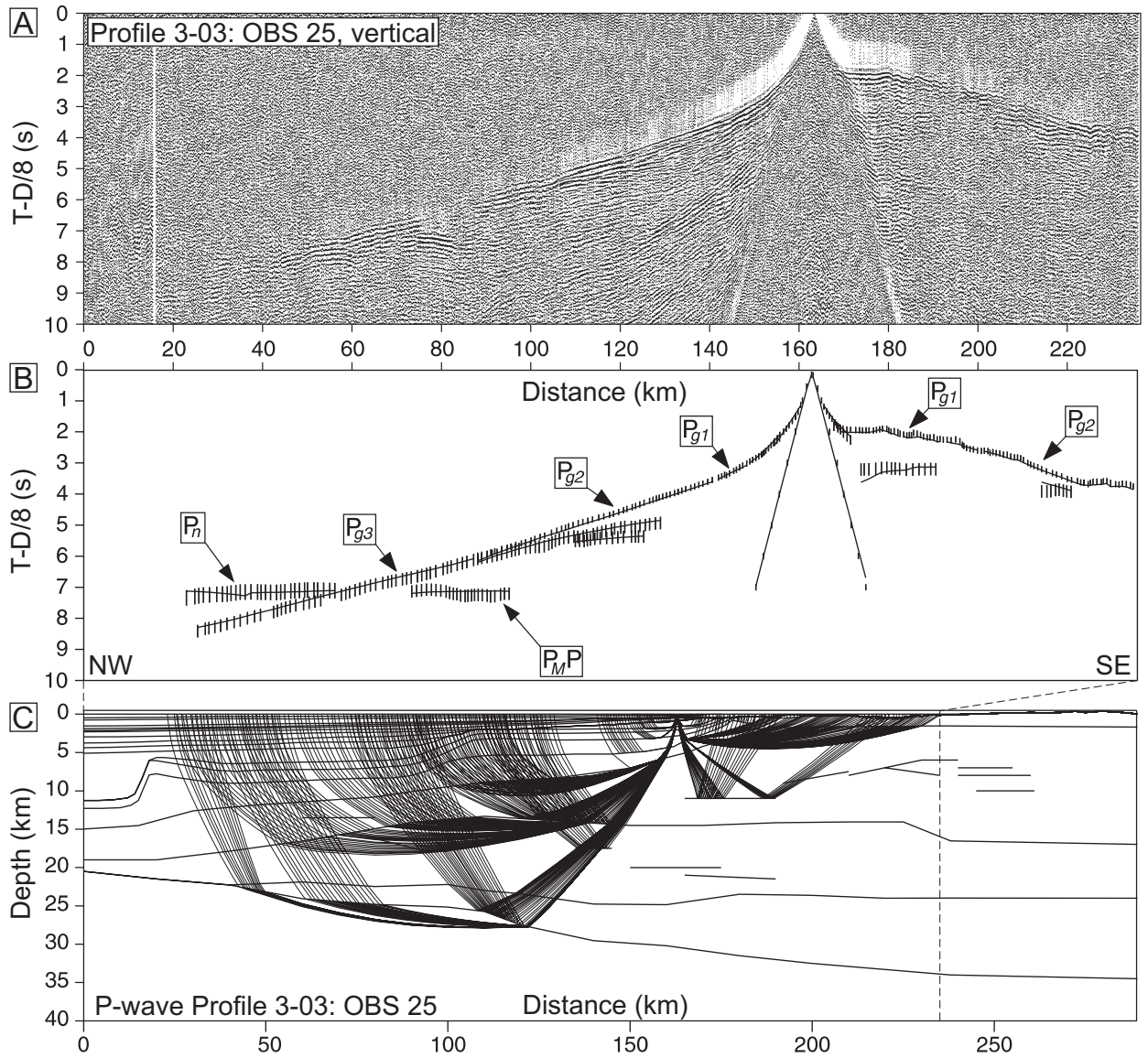
Fig. 28. OBS 25, Profile 3-03. A: OBS data, vertical component. B: Interpretation (vertical bars) and model travel-time (lines) fit. C: Ray-tracing of the velocity model.

Fig. 29. OBS 24, Profile 3-03. A: OBS data, vertical component. B: Interpretation (vertical bars) and model travel-time (lines) fit. C: Ray-tracing of the velocity model.
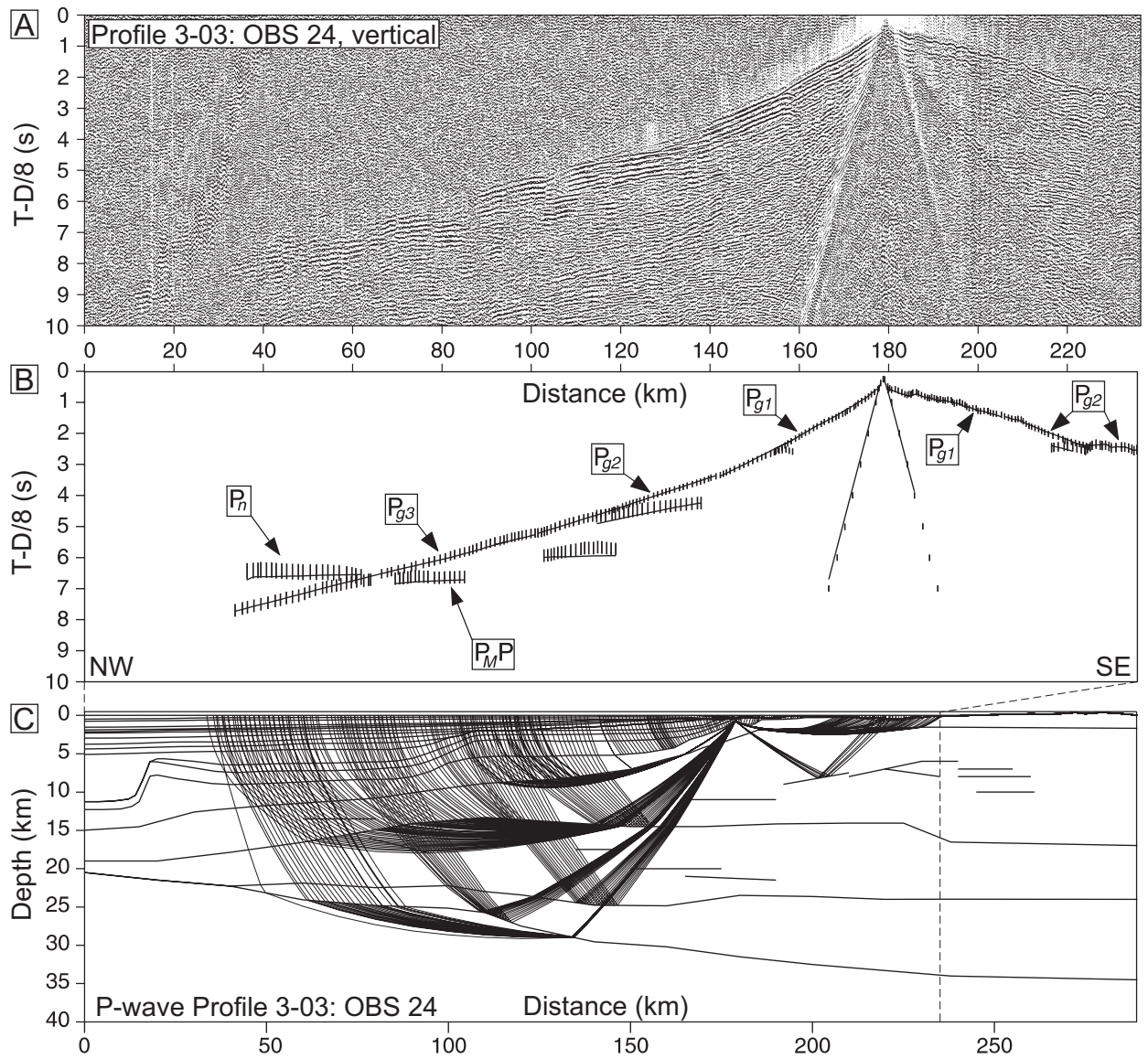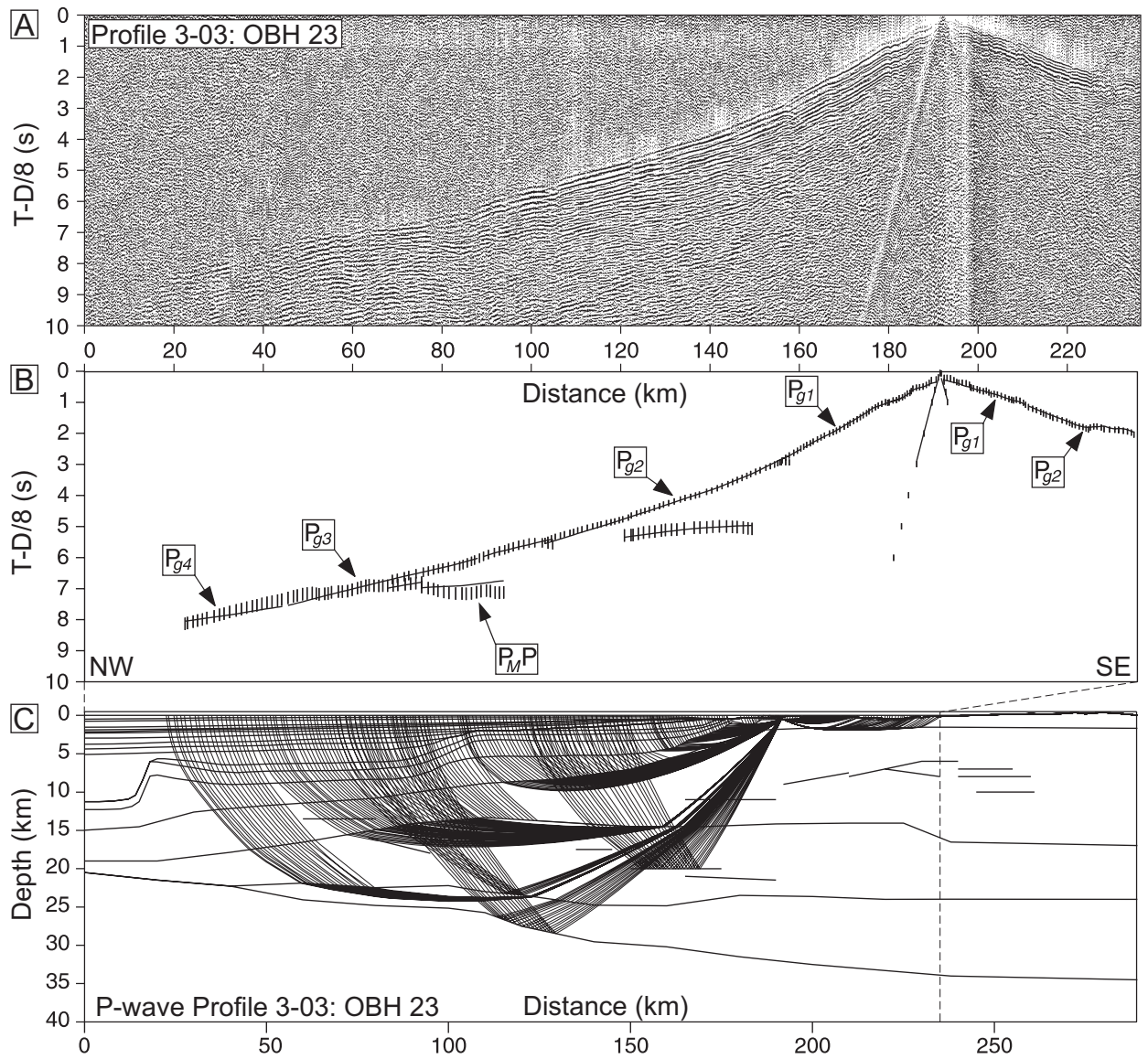
Fig. 30. OBH 23, Profile 3-03. A: Hydrophone data. B: Interpretation (vertical bars) and model travel-time (lines) fit. C: Ray-tracing of the velocity model.
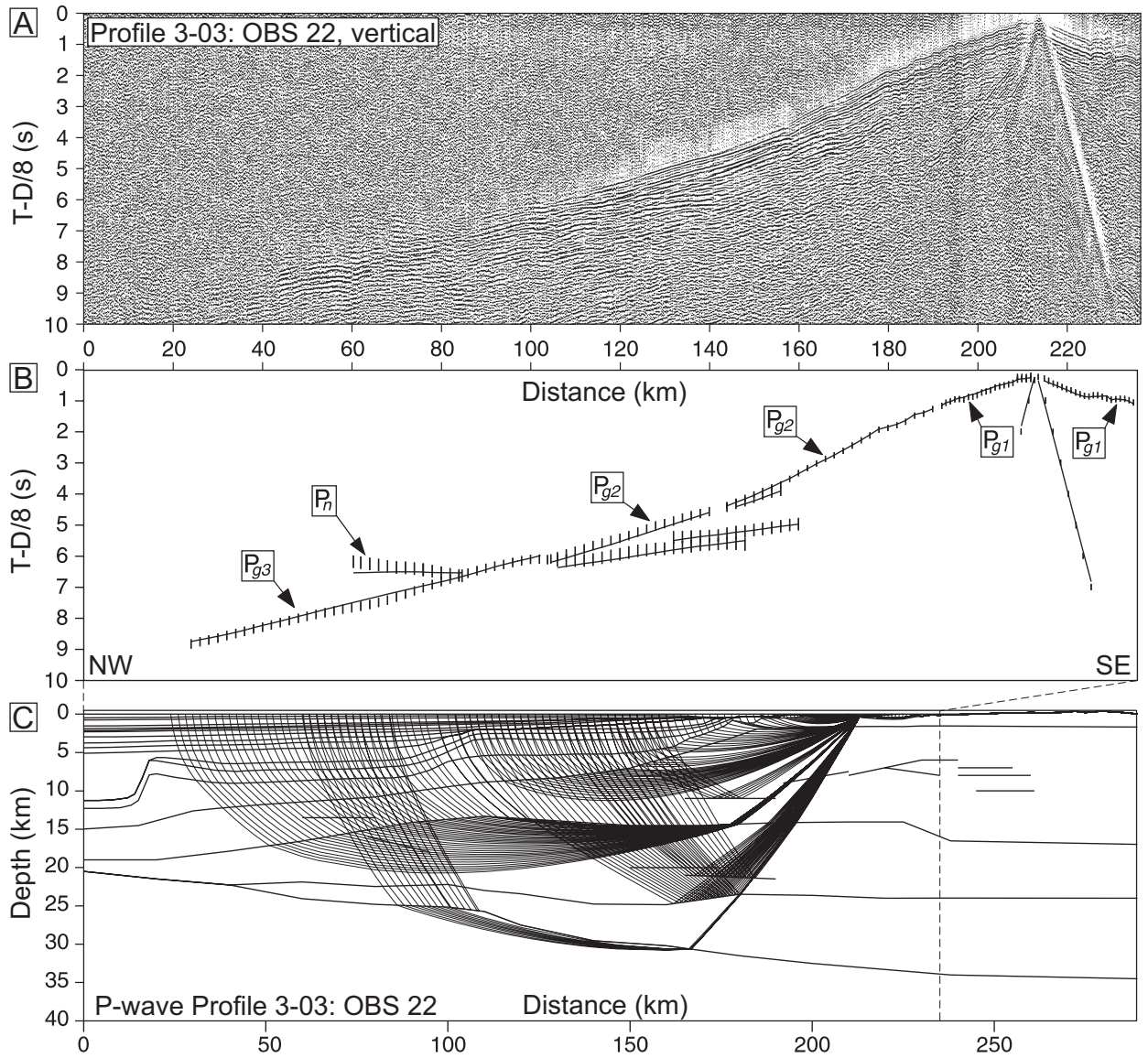
Fig. 31. OBS 22, Profile 3-03. A: OBS data, vertical component. B: Interpretation (vertical bars) and model travel-time (lines) fit. C: Ray-tracing of the velocity model.
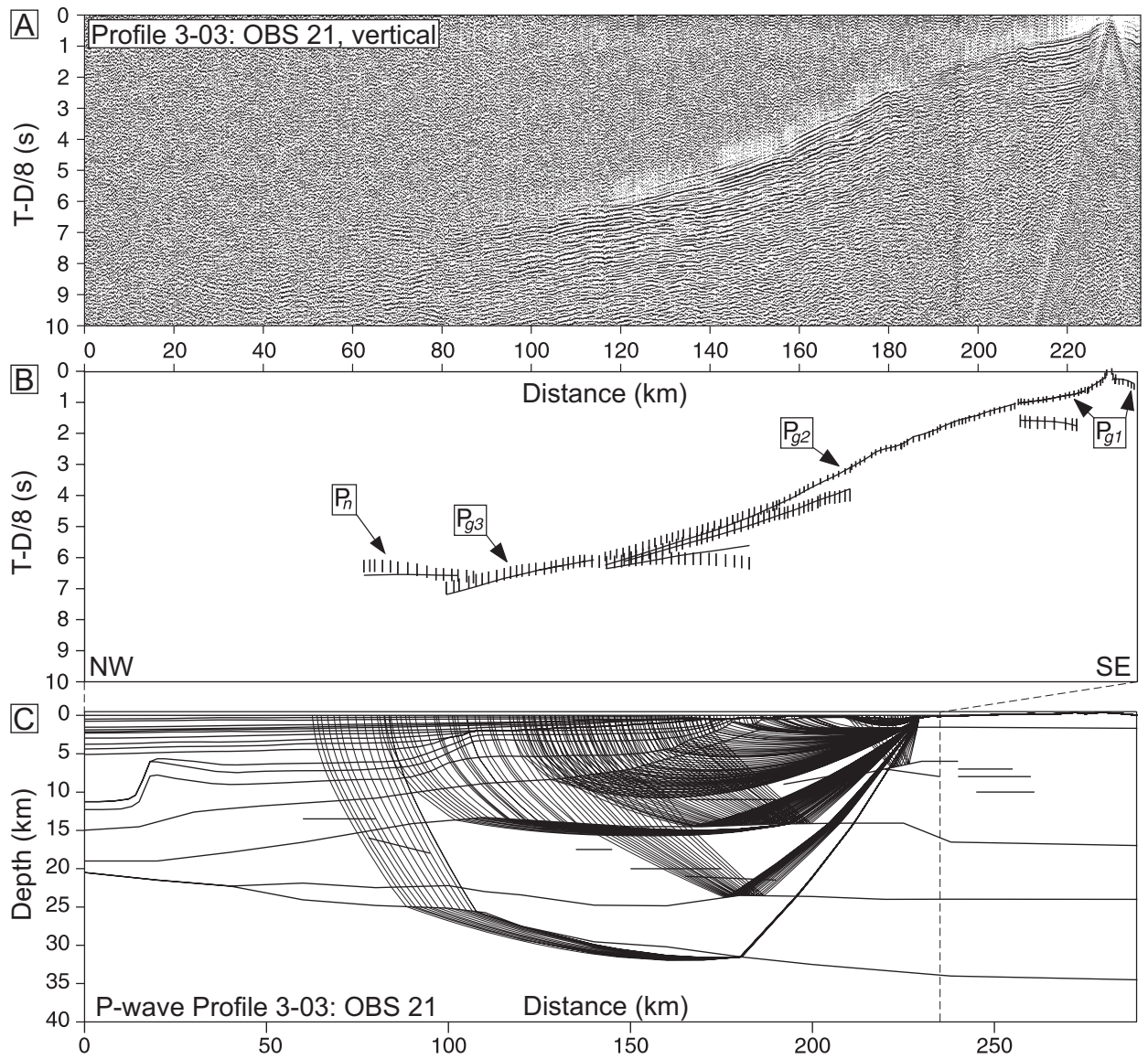
Fig. 32. OBS 21, Profile 3-03. A: OBS data, vertical component. B: Interpretation (vertical bars) and model travel-time (lines) fit. C: Ray-tracing of the velocity model.

Fig. 33. Land station 2, Profile 3-03. A: Seismometer data, vertical component. B: Interpretation (vertical bars) and model travel-time (lines) fit. C: Ray-tracing of the velocity model.

34

Fig. 34. Land station 3, Profile 3-03. A: Seismometer data, vertical component. B: Interpretation (vertical bars) and model travel-time (lines) fit. C: Ray-tracing of the velocity model.

Fig. 35. Land station 6, Profile 3-03. A: Seismometer data, vertical component. B: Interpretation (vertical bars) and model travel-time (lines) fit. C: Ray-tracing of the velocity model.
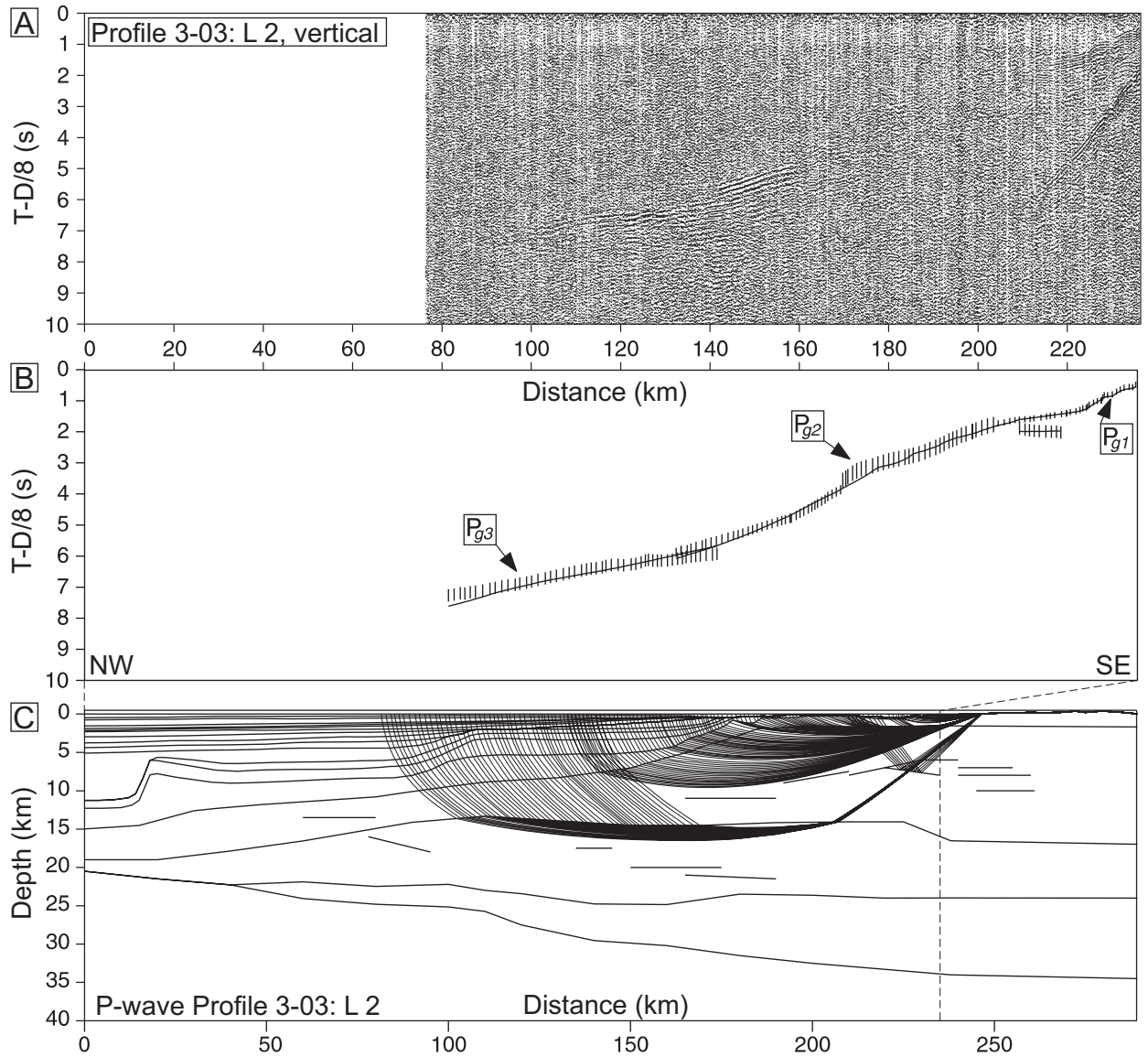
Fig. 36. Land station 8, Profile 3-03. A: Seismometer data, vertical component. B: Interpretation (vertical bars) and model travel-time (lines) fit. C: Ray-tracing of the velocity model.
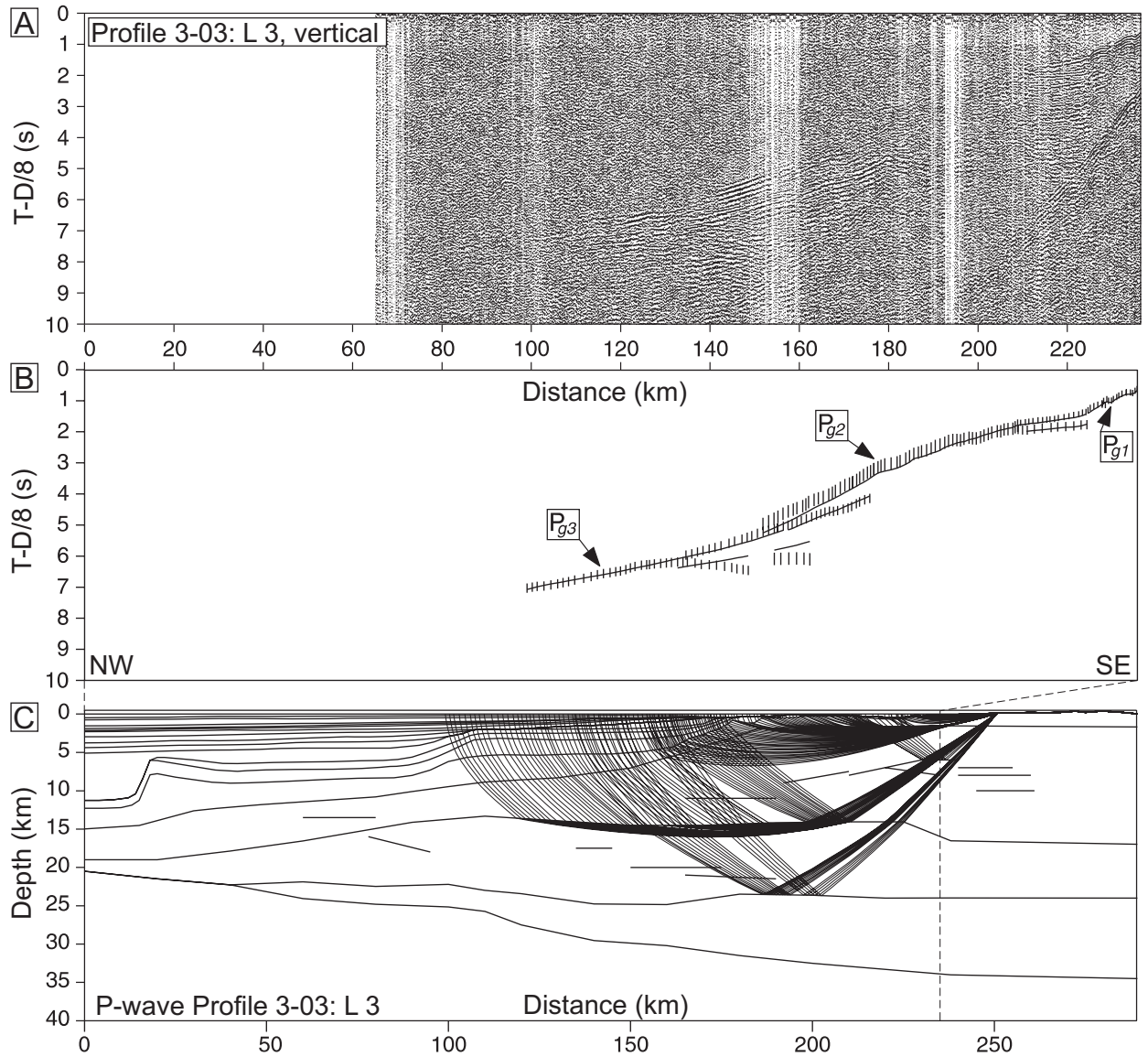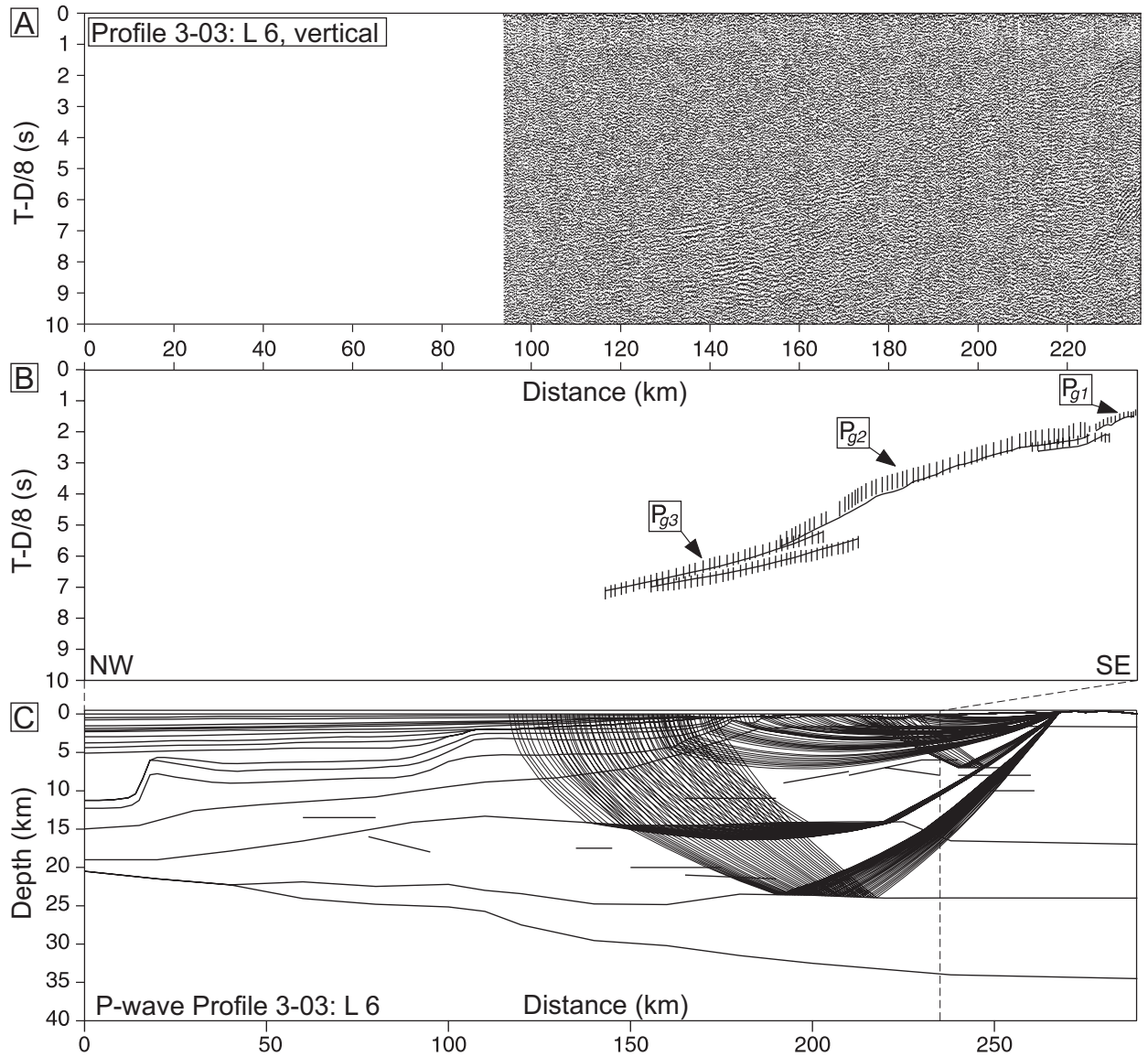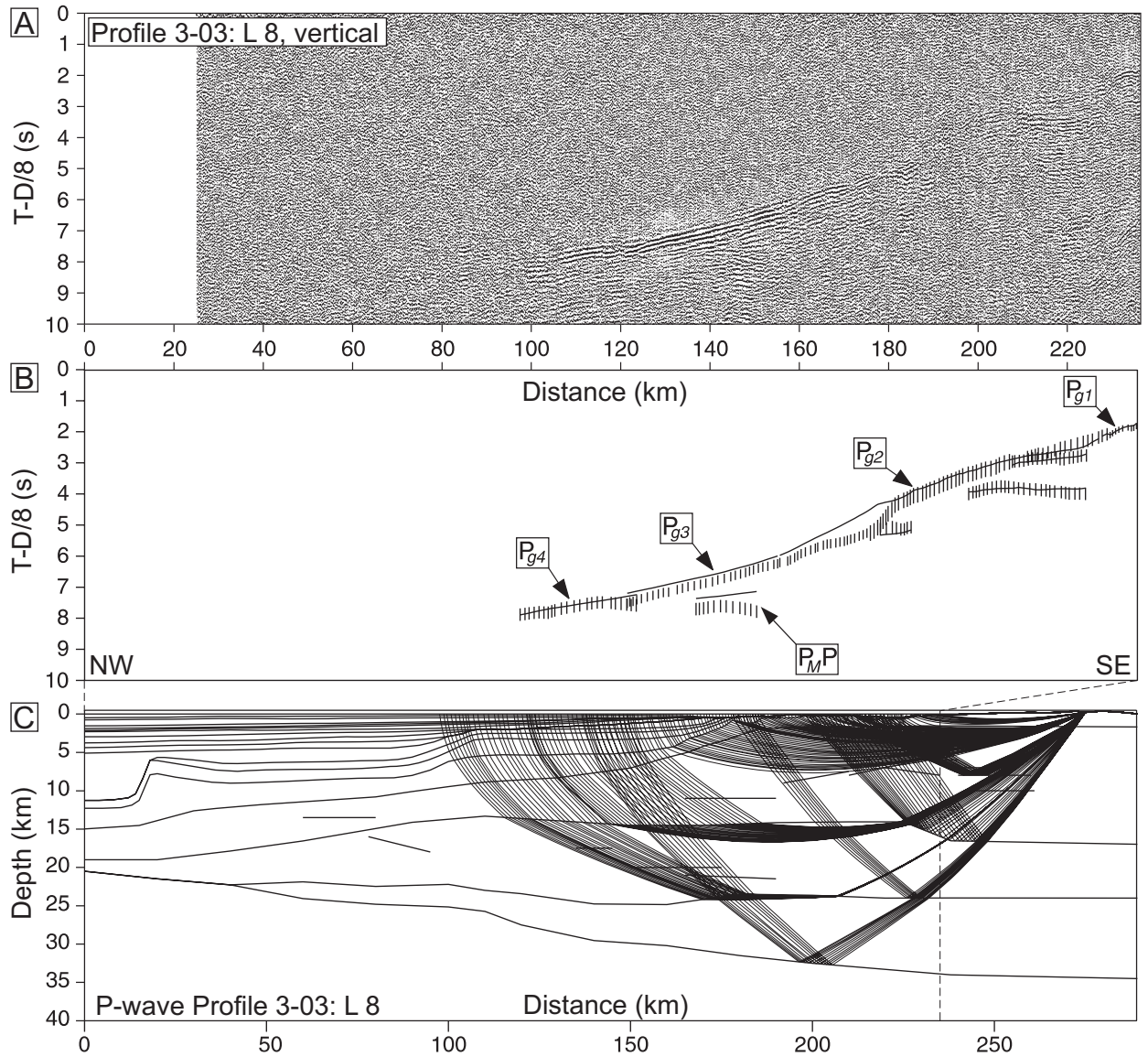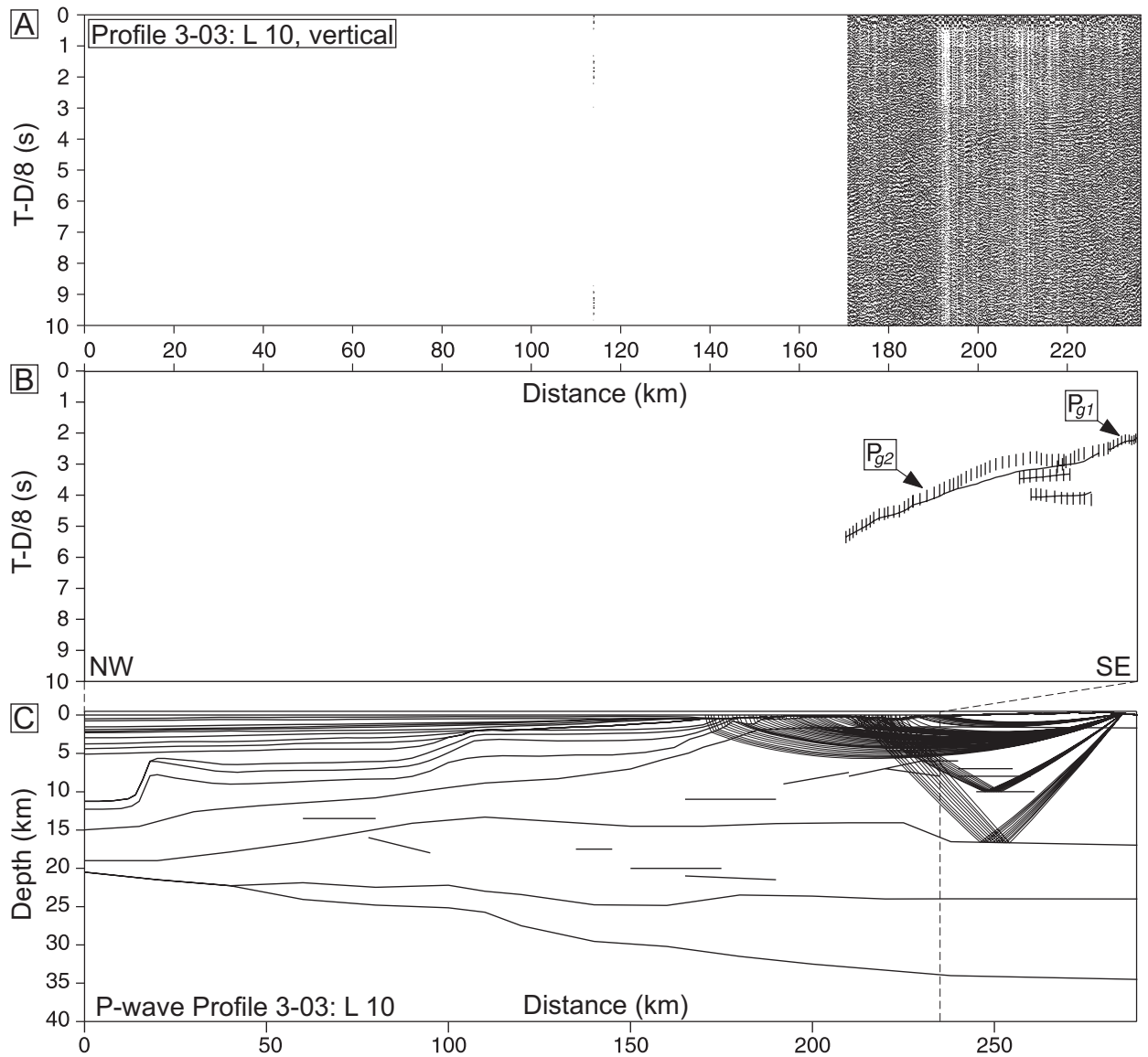
37

Fig. 37. Land station 10, Profile 3-03. A: Seismometer data, vertical component. Part of the data was lost due to recording failure. B: Interpretation (vertical bars) and model travel-time (lines) fit. C: Ray-tracing of the velocity model.
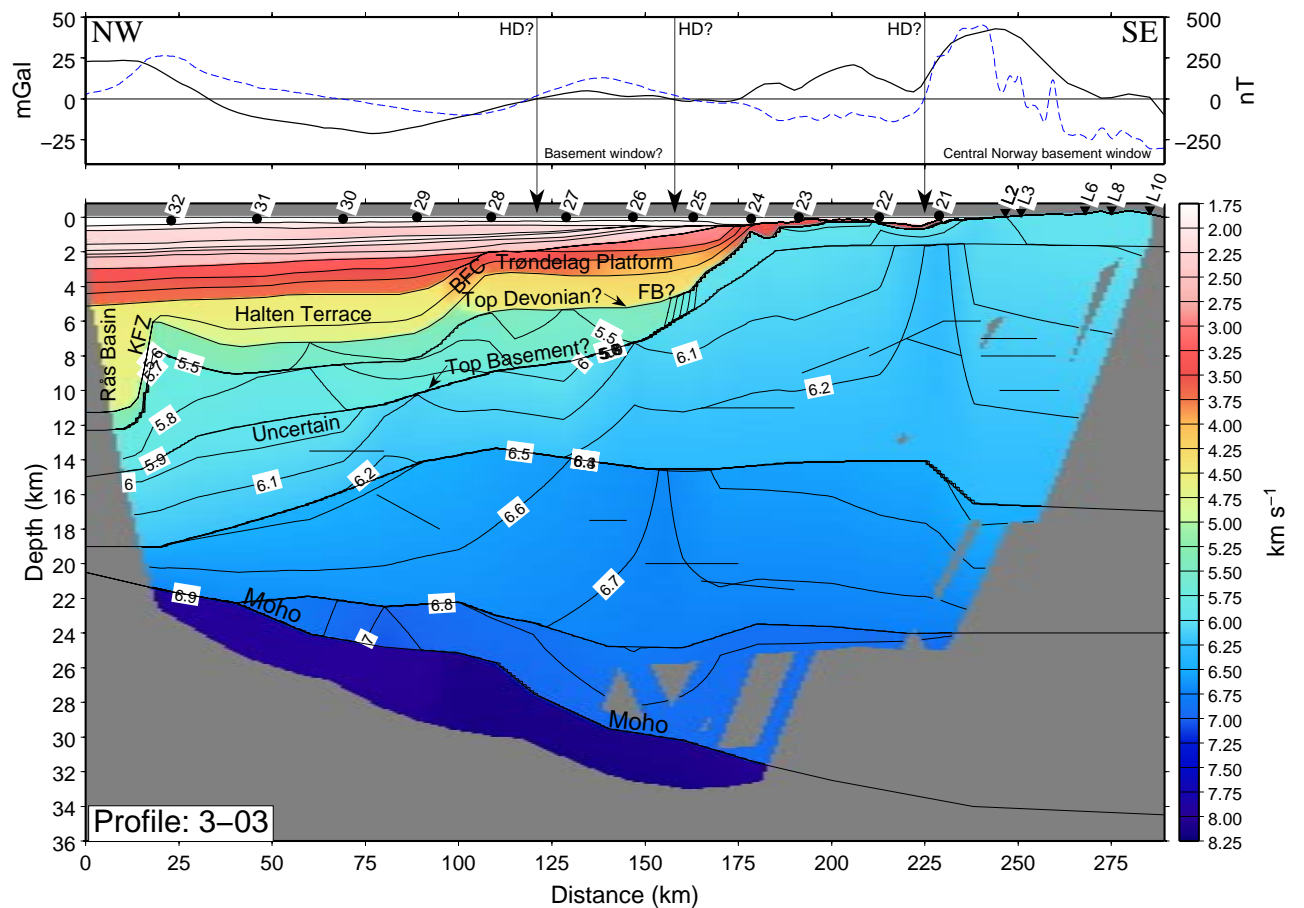
Fig. 38. Upper panel: Observed gravity (heavy line), magnetic anomalies (dashed blue line) along Profile 3-03. Lower panel: Gridded crustal velocity model of Profile 3-03. The parts of the model not covered by rays are masked. Floating reflectors are not included in the ray-coverage. Contour interval within the basement is 0.1 km s^{-1}. The intersection of the profile (Fig. 2) with the proposed offshore extension of the Høybakken Detachment (HD) (Skilbrei et al., 2002) is indicated. BFC: Bremstein Fault Complex, FB: Froan Basin, KFC: Klakk Fault Complex.

39

Modeling fit statistics

Summary of underground ray coverage (Fig. 39). High ray hit counts indicate well constrained parts of the models. The fits to individual phases constraining the basement part of the models are listed in Tab. 1.
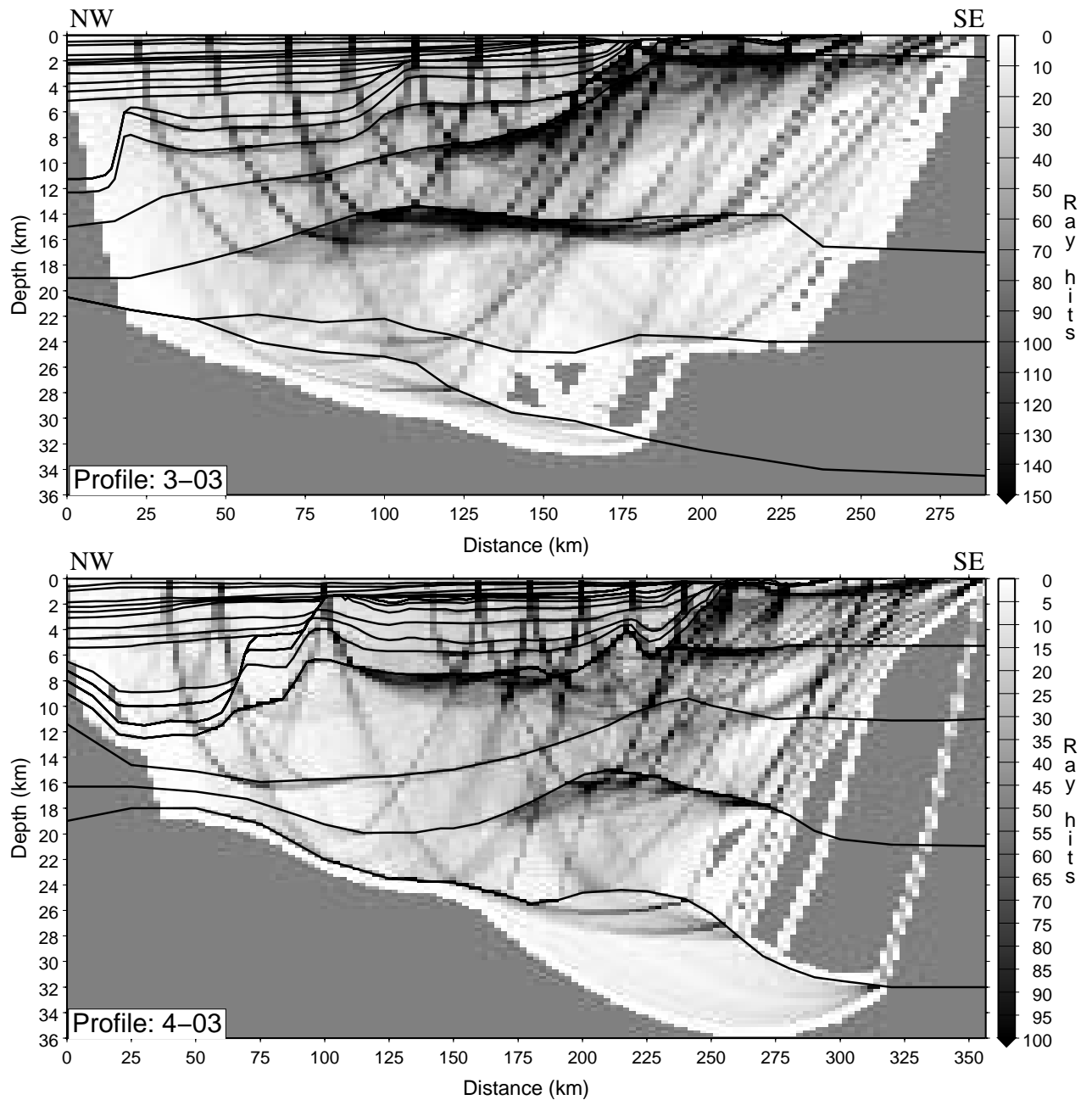

Fig. 39. Ray hit count for 2.5x0.25 km grid cell size for Profile 3-03 and 4-03. Reflections from floating reflectors do not constrain velocity and are not included.

Profile 3-03	Data points	RMS ΔT (ms)	Normalized χ^2
Sedimentary strata	528	75	0.595
Crystalline basement (incl. $P_M P$)	3263	143	0.730
Moho and upper mantle ($P_M P$ & P_n)	328	201	0.995
Profile 4-03	Data points	RMS ΔT (ms)	Normalized χ^2
Sedimentary strata	607	86	0.862
Crystalline basement (incl. $P_M P$)	2424	134	0.929
Moho and upper mantle ($P_M P$ & P_n)	519	135	0.779

Table 1
Fit statistics for the phases constraining main parts of the velocity models.

References

Blystad, P., Brekke, H., Færseth, R. B., Larsen, B. T., Skogseid, J. & Tørudbakken, B. 1995: Structural elements of the Norwegian continental shelf; Part II: the Norwegian Sea Region. *Norwegian Petroleum Directorate Bulletin 8*, 45 pp.

Olesen, O., Lundin, E., Nordgulen, Ø., Osmundsen, P. T., Skilbrei, J. R., Smethurst, M. A., Solli, A., Bugge, T. & Fichler, C. 2002: Bridging the gap between the onshore and offshore geology in Nordland, northern Norway. *Norwegian Journal of Geology 82*, 243–262.

Skilbrei, J. R., Kihle, O., Olesen, O., Gellein, J., Sindre, A., Solheim, D. & Nyland, B. 2000: *Gravity anomaly map, Norway and adjacent areas, scale 1:3 million.* Map and digital data, Geological Survey of Norway, Trondheim, Norway.

Skilbrei, J. R., Olesen, O., Osmundsen, P. T., Kihle, O., Aaro, S. & Fjellanger, E., 2002. A study of basement structures and onshore-offshore correlations in Central Norway. *Norwegian Journal of Geology 82*, 263–280.